THE EUROPEAN
PHYSICAL JOURNAL C

CrossMark

Measurement of differential cross sections for inclusive isolated-photon and photon+jet production in proton-proton collisions at $\sqrt{s} = 13$ TeV

CMS Collaboration[*]

CERN, 1211 Geneva 23, Switzerland

Abstract Measurements of inclusive isolated-photon and photon+jet production in proton–proton collisions at $\sqrt{s} = 13$ TeV are presented. The analysis uses data collected by the CMS experiment in 2015, corresponding to an integrated luminosity of 2.26 fb^{-1}. The cross section for inclusive isolated photon production is measured as a function of the photon transverse energy in a fiducial region. The cross section for photon+jet production is measured as a function of the photon transverse energy in the same fiducial region with identical photon requirements and with the highest transverse momentum jet. All measurements are in agreement with predictions from next-to-leading-order perturbative QCD.

1 Introduction

The measurement of inclusive isolated-photon and photon+jet production cross sections can directly probe quantum chromodynamics (QCD). The dominant production processes in proton–proton (pp) collisions at the energies of the CERN LHC are quark–gluon Compton scattering $qg \rightarrow q\gamma$, together with contributions from quark-antiquark annihilation $q\bar{q} \rightarrow g\gamma$, and parton fragmentation $q\bar{q}(gg) \rightarrow X + \gamma$. Both the CMS and ATLAS Collaborations have reported measurements of the differential cross sections for isolated prompt photon production [1–7] and for the production of a photon in association with jets [8–10] using data with center-of-mass energies of 2.76, 7, and 8 TeV. The ATLAS Collaboration has also reported the same measurements at a center-of-mass energy of 13 TeV [11,12].

The published measurements show agreement with the results of next-to-leading-order (NLO) perturbative QCD calculations [13,14].

These LHC measurements are sensitive to the gluon density function $g(x, Q^2)$ over a wide range of parton momentum fraction x and energy scale Q^2 [15–17]. These mea-

surements were not included in the global parton distribution function (PDF) fits [18–20] until very recently [21]. An improved understanding of all PDFs is key to reducing the associated theoretical uncertainties in the calculation of many relevant cross sections, including Higgs boson production and new physics searches.

In this paper, measurements are reported for the inclusive isolated-photon cross section in a fiducial region using data collected by the CMS Collaboration in proton-proton collisions at $\sqrt{s} = 13$ TeV, corresponding to an integrated luminosity of 2.26 fb^{-1} [22]. The specific fiducial region is defined at generator level as: (1) photon transverse momentum $E_T > 190$ GeV, (2) rapidity $|y| < 2.5$, and (3) an isolated photon where the sum of the p_T of all particles inside a cone of radius $\Delta R = \sqrt{(\Delta\phi)^2 + (\Delta\eta)^2} = 0.4$ around the photon is less than 5 GeV. The photon+jet cross section is also measured in this fiducial region with the same photon requirements and with $p_T^{jet} > 30$ GeV and $|y^{jet}| < 2.4$. The significant increase in center-of-mass energy compared with the previous CMS papers [1,2] opens a large additional region of phase space.

The dominant background for the photon+jet process is QCD multijet production with an isolated electromagnetic (EM) deposit from decays of neutral hadrons, mostly from π^0 mesons. A multivariate analysis method is used to identify prompt photons using a boosted decision tree (BDT) algorithm, implemented using the TMVA v4.1.2 toolkit [23]. Photon yields are extracted using the shape of the BDT distributions, and the measured cross sections are compared to the results of NLO QCD calculations.

2 The CMS detector

CMS is a general-purpose detector built to explore physics at the TeV scale. The central feature of the CMS apparatus is a superconducting solenoid of 6 m internal diameter, pro-

Springer

viding a magnetic field of 3.8 T. Within the solenoid volume are a silicon pixel and a strip tracker, a lead tungstate crystal electromagnetic calorimeter (ECAL), and a brass and scintillator hadron calorimeter (HCAL), each composed of a barrel and two endcap sections. Forward calorimeters extend the pseudorapidity η coverage provided by the barrel and endcap detectors. Muons are measured in gas-ionization detectors embedded in the steel flux return yoke outside the solenoid. A more detailed description of the CMS detector, together with the definition of the coordinate system and the relevant kinematic variables, is given in Ref. [24].

The ECAL consists of 75 848 lead tungstate crystals, which provide coverage up to $|\eta| = 1.479$ in the barrel region (EB) and $1.479 < |\eta| < 3.0$ in two endcap regions (EE). A preshower detector consisting of two planes of silicon sensors interleaved with a total of 3 radiation lengths of lead is located in front of the EE.

The silicon tracker measures charged particles within the range $|\eta| < 2.5$. For nonisolated particles of transverse momenta $1 < p_T < 10$ GeV and $|\eta| < 1.4$, the track resolutions are typically 1.5% in p_T and 25–90 (45–150) μm in the transverse (longitudinal) impact parameter [25].

The global event reconstruction (also called particle-flow event reconstruction) [26] reconstructs and identifies each particle candidate with an optimized combination of all subdetector information.

In CMS, both converted and unconverted photons are reconstructed using ECAL clusters and are included in the analysis. The clustering algorithm results in an almost complete collection of the energy of the photons, unconverted ones and those converting in the material upstream of the calorimeter. First, cluster "seeds" are identified as local energy maxima above a given threshold. Second, clusters are grown from the seeds by aggregating crystals with at least one side in common with a clustered crystal and with an energy in excess of a given threshold. This threshold represents about two standard deviations of the electronic noise, which depends on $|\eta|$. The energy in an individual crystal can be shared between clusters under the assumption that each seed corresponds to a single EM particle. Finally, clusters are merged into "superclusters", to allow good energy containment, accounting for geometrical variations of the detector along η, and increasing robustness against additional pp collisions in the same or adjacent bunch crossings (pileup). The clustering excludes $1.44 < |\eta| < 1.56$, which corresponds to the transition region between the EB and EE. The fiducial region terminates at $|\eta| = 2.5$ where the tracker coverage ends.

The energy of photons is computed from the sum of the energies of the clustered crystals, calibrated and corrected for degradation in the crystal response over time [27]. The preshower energy is added to that of the superclusters in the region covered by this detector. To optimize the resolution, the photon energy is corrected using a multivariate regression technique that estimates the containment of the electromagnetic shower in the superclusters, the shower losses for photons that convert in the material upstream of the calorimeter, and the effects of pileup [28]. The regression training is performed on simulated events using shower shape and position variables of the photon as inputs. The regression provides a per-photon estimate of the function parameters that quantify the containment, the shower losses, and pileup and therefore a prediction of the distribution of the ratio of true energy to the uncorrected supercluster energy. The most probable value of this distribution is taken as the photon energy correction. The regression output is used to correct the reconstucted photon energy in data to agree with simulated events. An additional smearing is applied to the photon energy in simulation to reproduce the resolution observed in data. The scale correction and smearing procedure uses a multistep procedure exploiting electrons from $Z \rightarrow e^+e^-$ decays. In the EB, an energy resolution of about 1% is achieved for unconverted photons in the tens of GeV energy range. The remaining EB photons have a resolution of about 1.3% up to $|\eta| = 1.0$, rising to about 2.5% at $|\eta| = 1.4$. In the EE, the resolution of unconverted or late-converting photons is about 2.5%, while the remaining EE photons have a resolution between 3 and 4%.

Electrons are identified as a primary charged track consistent with potentially multiple ECAL energy clusters from both the electron and from potential bremsstrahlung photons produced in the tracker material. Muons are identified as a track in the central tracker consistent with either a track or several hits in the muon system, associated with a minimum ionization signature in the calorimeters. Charged hadrons are charged-particle tracks not identified as electrons or muons. Finally, neutral hadrons are identified as HCAL energy clusters not linked to any charged-hadron track, or as ECAL and HCAL energy excesses with respect to the expected charged-hadron energy deposit.

Jets are clustered from all particle candidates reconstructed by the global event reconstruction with the infrared- and collinear- safe anti-k_T algorithm [29,30] using a distance parameter R of 0.4. The momenta of jets reconstructed using particle-flow candidates in the simulation are within 5 to 10% of particle-level jet momenta over the whole jet p_T spectrum and detector acceptance, and corrected on average accordingly. In situ measurements of the momentum balance in dijet, photon+jet, Z+jet, and multijet events are used to correct for any residual differences in jet energy scale in data and simulation [31]. The jet energy resolution amounts typically to 15 (8)% at 10 (100) GeV.

3 Simulation samples

Simulated event samples for photon+jet and multijet final states are generated at leading order (LO) with PYTHIA 8 (v8.212) [32]. The photon+jet sample contains direct photon production originating from quark–gluon Compton scattering and quark-antiquark annihilation.

The multijet sample, which is dominated by final states with quark and gluon jets, is used in the estimate of systematic uncertainties, and to estimate the small bias in the extracted photon yield from the BDT fit, as described in Sect. 5. For these studies, events containing a photon, produced via the fragmentation process and passing the fiducial requirements, are removed, leaving only events with nonfiducial photons. The removed events are considered part of the signal, although they are not included in the signal sample in the training of the BDT due to associated large statistical uncertainties. The distributions of the variables used in the BDT training were examined and are consistent with those of the direct photons, within the statistical uncertainty.

The MADGRAPH (v5.2.2.2) [33,34] LO generator, interfaced with PYTHIA 8, is used to generate an additional sample of photon+jet events containing up to 4 jets that are used to estimate systematic uncertainties. Samples of Z/γ^*+jets events are generated at NLO with MADGRAPH5_aMC@NLO (v5.2.2.2) [33,35] and are used for calibration and validation studies described later. The CUETP8M1 tune [36] is used in PYTHIA 8. The NNPDF2.3 LO PDF [37] and the NNPDF3.0 NLO PDF [18] are used to generate simulation samples, where the former is used with PYTHIA 8.

The simulated processes include the effect of the pileup. The pileup contribution is simulated with additional minimum bias events superimposed on the primary event using the measured distribution of the number of reconstructed interaction vertices, an average of 14 vertices per bunch crossing. A detailed detector simulation based on the GEANT4 (v9.4p03) [38] package is applied to all the generated signal and background samples.

4 Data samples and event selection criteria

Events containing high energy photon candidates are selected using the two-level CMS trigger system [39]. At the first level, events are accepted if they have an ECAL trigger tower, which has a segmentation corresponding to 5×5 ECAL crystals, with total transverse energy E_T, defined as the magnitude of the photon transverse momentum, greater than 40 GeV. The second level of the trigger system uses the same reconstruction algorithm as the offline photon reconstruction [28]. An event is accepted online if it contains at least one ECAL cluster with E_T greater than 175 GeV, and

if the "H/E", defined as the ratio of energy deposited in the HCAL to that in the ECAL, is less than 0.15 (0.10) in the EB (EE) region.

All events are required to have at least one well-reconstructed primary vertex [25]. The reconstructed vertex with the largest value of summed physics-object p_T^2 is the primary pp interaction vertex. The physics objects are the jets, clustered using the jet finding algorithm [29,30] with the tracks assigned to the vertex as inputs, and the associated missing transverse momentum p_T^{miss} [40], taken as the negative vector sum of the p_T of those jets. In addition, photon+jet events are required to be balanced in p_T, and hence the magnitude of missing transverse momentum, defined as the magnitude of the negative vector sum of the momenta of all reconstructed particle-flow objects projected onto the plane perpendicular to the beam axis in an event, is required to be less than 70% of the highest photon E_T.

Photon candidates are selected as described in the following procedure. An electron veto is imposed by requiring the absence of hits in the innermost layer of the silicon pixel detector that could be ascribed to an electron track consistent with the energy and position of the photon ECAL cluster. Criteria on the energy measured in HCAL (H), isolation, and shower shape variables are applied to reject photons arising from electromagnetic decays of particles in hadronic showers. Hence, H/E is required to be less than 0.08 (0.05) for photon candidates in the EB (EE), respectively. The sum of the E_T of other photons in a cone (photon isolation) of size $\Delta R = 0.3$ around the photon candidate is required to be less than 15 GeV, and the sum of p_T of charged hadrons in the same cone (hadron isolation) is required to be less than 2.0 (1.5) GeV for photon candidates in the EB (EE).

To further suppress photons from decays of neutral mesons (π^0, η, etc.) that survive the isolation and HCAL energy leakage criteria, a selection on the EM shower shape is imposed by requiring that its second moment $\sigma_{\eta\eta}$ [28], which is a measure of the lateral extension of the shower along the η direction, be $<0.015 (0.045)$ for photon candidates in the EB (EE). The photon candidate with the highest E_T that satisfies the above selection criteria in each event is referred to as the leading photon. The data consist of 212 134 events after applying inclusive isolated-photon selections and 207 120 events after applying the photon+jet requirements. The estimated electron contribution is typically at 10^{-3} level as a result of the electron veto algorithm. This contribution is small compared to statistical uncertainties of the photon yield and other systematic uncertainties.

The photon reconstruction and selection efficiencies are estimated using simulated events that pass the fiducial region requirements at the generator level. The efficiency is about 90–92% (83–85%) for EB (EE) photons, depending on the E_T of the photon candidate. The loss of efficiency comes primarily from the hadron isolation requirement. Multiplica-
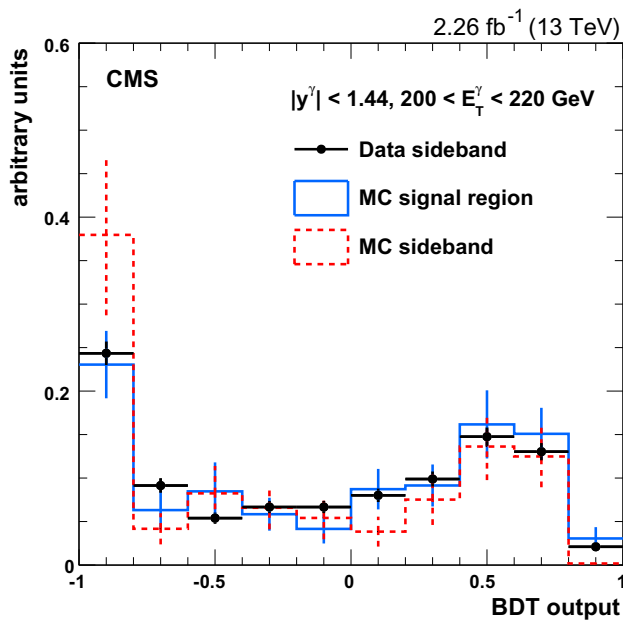
Fig. 1 Distributions of the BDT for background photons in the 200–220 GeV bin for the EB region. The points show events from a sideband region of the photon isolation selection criteria, the solid histogram shows the events in the signal region in simulated QCD multijet events, and the dashed histogram shows the sideband region for simulated QCD multijet events. All three samples have their statistical uncertainties shown as error bars

tive scale factors (SF) are applied to correct potential differences in efficiencies between data and simulation. The SFs are obtained from the ratio of the efficiency in data to that in simulated control samples. The photon SF is derived from Drell–Yan $Z \to e^+e^-$ events, where one of the electrons is reconstructed as a photon. The events are selected by requiring the invariant mass of the electron pair to be between 60 and 120 GeV. The electron veto SF is determined using final-state radiation photons in $Z \to \mu^+\mu^-\gamma$ events. All SFs are within 1% of unity, and their uncertainties are included in the total systematic uncertainty. All efficiencies and SF are measured as functions of photon E_T and rapidity y using the same binning as the cross section measurement.

The absolute photon trigger efficiency, as a function of photon E_T, is measured using events collected with a jet trigger that contains a photon candidate, which satisfies the signal selection criteria and is spatially separated from the jet that triggered the event by $\Delta R(\gamma, \text{jet}) > 0.7$. The trigger efficiency is above 99% for EB (EE) photons above 200 (220) GeV. The E_T-dependent trigger efficiency is used to compute the cross section, and the associated uncertainties are incorporated into the uncertainty calculation for the cross section.

For the cross section measurement as a function of jet y, the jets are required to: (1) satisfy a set of selection criteria
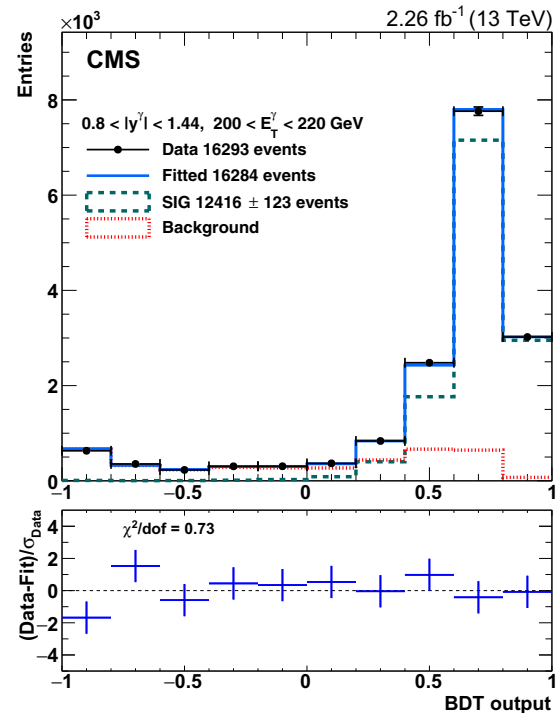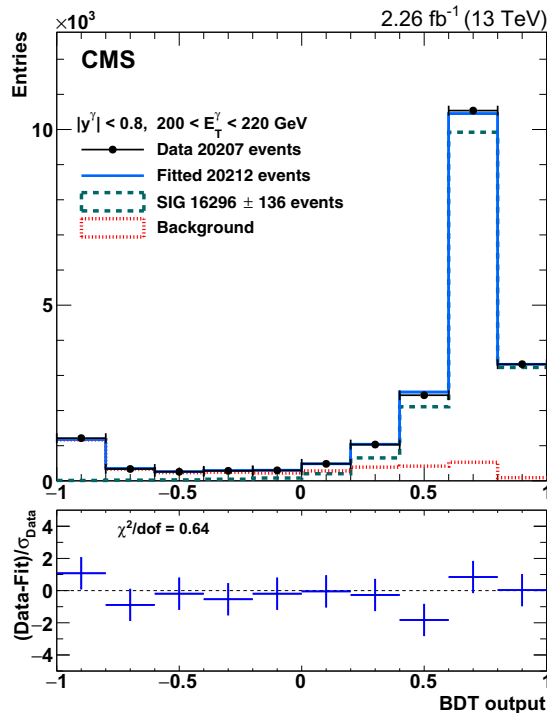

Fig. 2 Distributions of the BDT output for an EB (left) and an EE (right) bin with photon E_T between 200 and 220 GeV and $|y^{\text{jet}}| < 1.5$. The points represent data, and the solid histograms, approaching the data points, represent the fit results with the signal (dashed) and background (dotted) components displayed. The bottom panels show the ratio of the data to the fitted results and the χ^2/dof

Table 1 Impact on cross sections, in percent, for each systematic uncertainty source in the four photon rapidity regions, $|y^\gamma| < 0.8$, $0.8 < |y^\gamma| < 1.44$, $1.57 < |y^\gamma| < 2.1$, and $2.1 < |y^\gamma| < 2.5$. The ranges, when quoted, indicate the variation over photon E_T between 190 and 1000 GeV

Source	$|y^\gamma| < 0.8$	$0.8 < |y^\gamma| < 1.44$	$1.57 < |y^\gamma| < 2.1$	$2.1 < |y^\gamma| < 2.5$
Trigger efficiency	0.7–8.5	0.2–13.4	0.6–20.5	0.3–7.8
Selection efficiency	0.1–1.3	0.1–1.3	0.1–5.3	0.1–1.1
Data-to-MC scale factor	3.7	3.7	7.1	7.1
Template shape	0.6–5.0	0.1–10.2	0.5–4.9	0.6–16.2
Event migration	3.8–5.5	1.2–4.1	2.0–8.5	2.3–10.3
Total w/o luminosity	5.4–12.0	5.9–18.2	8.2–26.9	8.6–21.7
Integrated luminosity	2.3			

that remove detector noise [41], (2) have a separation from the leading photon of $\Delta R > 0.4$, and (3) have p_T greater than 30 GeV. The p_T requirement for jets is fully efficient for simulation events with both photon and jet in their fiducial regions. The jet candidate with the highest p_T satisfying the above requirements is selected.

The measurement of the differential cross section for inclusive isolated photons uses four ranges of photon rapidity, $|y^\gamma| < 0.8$, $0.8 < |y^\gamma| < 1.44$, $1.57 < |y^\gamma| < 2.1$, and $2.1 < |y^\gamma| < 2.5$. The photon+jet differential cross section measurement uses two ranges of photon rapidity, $|y^\gamma| < 1.44$ and $1.57 < |y^\gamma| < 2.5$, and two ranges of jet rapidity, $|y^{jet}| < 1.5$ and $1.5 < |y^{jet}| < 2.4$. For all cases, the results are presented in nine bins in photon E_T between 190 and 1000 GeV, except for two cases: the $2.1 < |y^\gamma| < 2.5$ region for the isolated-photon measurement and the $1.57 < |y^\gamma| < 2.5$ and $1.5 < |y^{jet}| < 2.4$ regions for the photon+jet measurement, where eight bins in photon E_T between 190 and 750 GeV are used.

5 Cross section measurement

To further suppress remaining backgrounds originating from jets faking photons, a BDT is constructed utilizing the following discriminating variables:

1. Photon η, ϕ, and energy;
2. Several shower shape variables:

   (a) The energy sum of the 3×3 crystals centered on the most energetic crystal in the photon divided by the energy of the photon;
   (b) The ratio of $E_{2\times2}$, the maximum energy sum collected in a 2×2 crystal matrix that includes the largest energy crystal in the photon, and $E_{5\times5}$, the energy collected in a 5×5 crystal matrix centered around the same crystal ($E_{2\times2}/E_{5\times5}$);
   (c) The second moment of the EM cluster shape along the η direction ($\sigma_{\eta\eta}$);
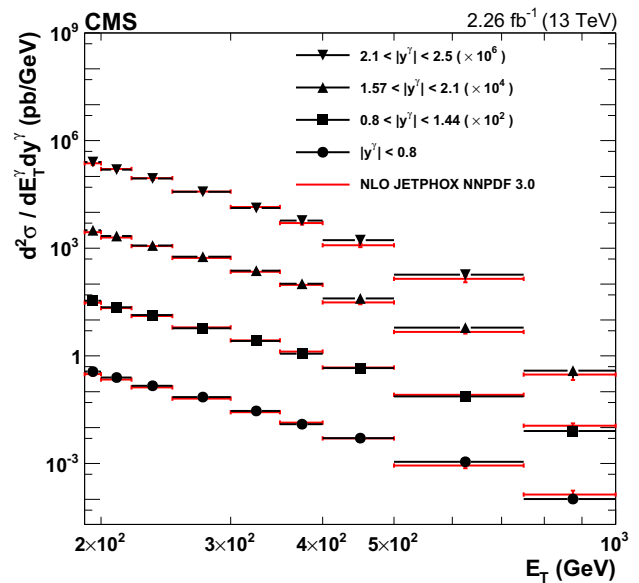

Fig. 3 Differential cross sections for isolated-photon production in photon rapidity bins, $|y^\gamma| < 0.8$, $0.8 < |y^\gamma| < 1.44$, $1.57 < |y^\gamma| < 2.1$, and $2.1 < |y^\gamma| < 2.5$. The points show the measured values and their total uncertainties; the lines show the NLO JETPHOX predictions with the NNPDF3.0 PDF set
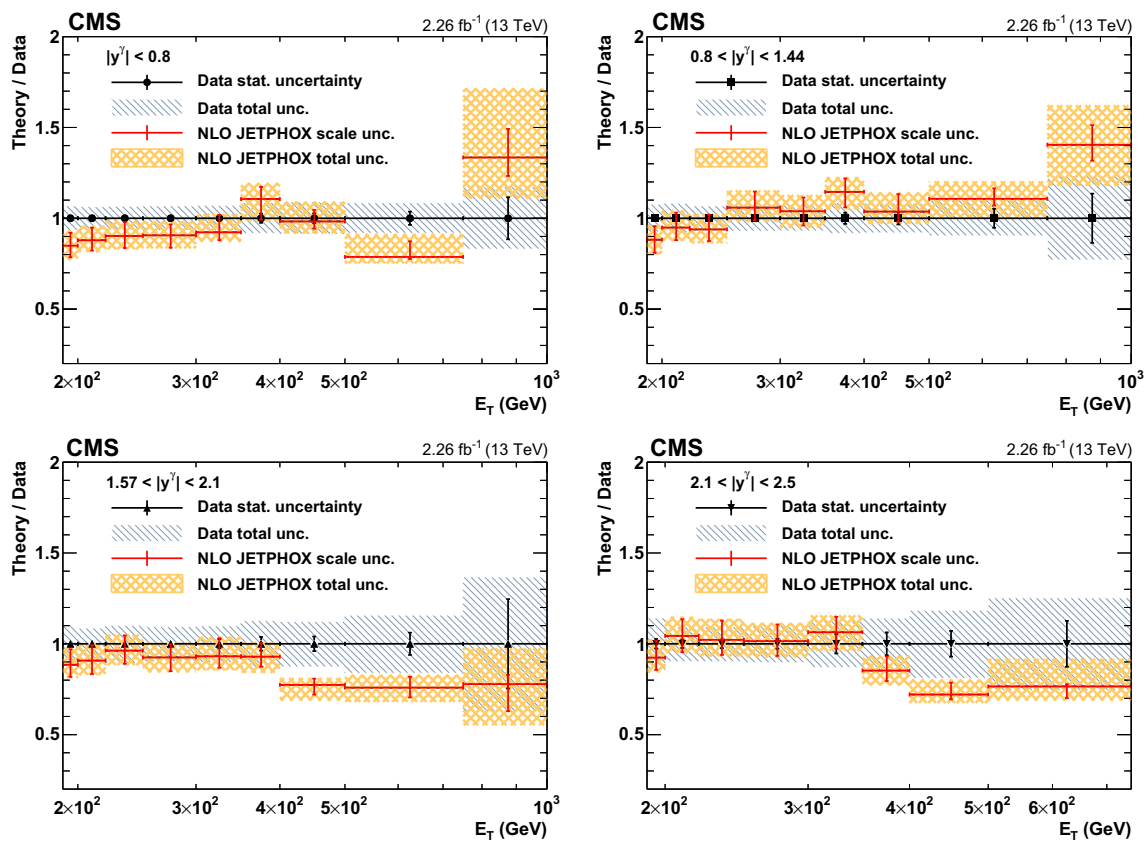
   (d) The diagonal component of the covariance matrix that is constructed from the energy-weighted crystal positions within the 5×5 crystal array ($q_{\eta\phi}$);
   (e) The energy-weighted spreads along η (σ_η) and ϕ (σ_ϕ), calculated using all crystals in the photon cluster, which provide further measures of the lateral spread of the shower.

3. For photon candidates in the EE, the preshower shower width, $\sigma_{RR} = \sqrt{\sigma_{xx}^2 + \sigma_{yy}^2}$, where σ_{xx} and σ_{yy} measure the lateral spread in the two orthogonal sensor planes of the detector, and the fraction of energy deposits in the preshower.
4. The median energy density per unit area in the event ρ [30] to minimize the effect of the pileup.

Fig. 4 The ratios of theoretical NLO predictions to data for the differential cross sections for isolated-photon production in four photon rapidity bins, $|y^\gamma| < 0.8$, $0.8 < |y^\gamma| < 1.44$, $1.57 < |y^\gamma| < 2.1$, and $2.1 < |y^\gamma| < 2.5$, are shown. The error bars on data points represent the statistical uncertainty, while the hatched area shows the total experimental uncertainty. The errors on the ratio represent scale uncertainties, and the shaded regions represent the total theoretical uncertainties

The distributions of the BDT values are used in a two-template binned likelihood fit to estimate the photon yield. A separate BDT is constructed for each bin of photon y and E_T. The signal BDT template is obtained from the sample of simulated photon+jet events generated using PYTHIA 8. This template is validated using $Z \rightarrow \mu^+\mu^-\gamma$ data samples and also a data sample of $Z \rightarrow e^+e^-$ candidates where each candidate contains an electron reconstructed as a photon. The signal templates have a systematic uncertainty due to differences in the distributions of the BDT input variables in data and simulation. To evaluate this uncertainty, the distribution of each variable obtained from a sample of simulated $Z \rightarrow e^+e^-$ events is modified until agreement is obtained with the data. Signal templates are made using the same procedure. The difference in the templates is treated as a nuisance parameter in the fit procedure.

The background BDT template is derived from the data, using a sideband region defined using the same signal selection, but relaxing the hadron isolation criterion. The hadron isolation for the sideband region is required to be between 7 and 13 (6 and 12) GeV for EB (EE) photons, where the chosen ranges ensure negligible signal contamination. Possible

biases in the photon yields due to differences between the background BDT templates in the control and signal regions are estimated using simulated events and are found to be less than 5%. Photon yields extracted from the fits are corrected for these biases. The statistical uncertainties in each bin of the background template constructed from the data sideband events are also included as nuisance parameters in the fitting procedure. Figure 1 shows the BDT templates obtained for a particular photon E_T and y bin for the data sideband and for the signal and sideband regions from simulated QCD multi-jet events. The distributions of BDT outputs for EB and EE photons in data are shown in Fig. 2 for photon E_T between 200 and 220 GeV and jet $|y| < 1.5$. The fitted results for the signal, background, and combined distributions are also shown in Fig. 2. The ratio of experimental data to the simulation results demonstrates agreement as indicated by the χ^2 per degree of freedom.

The corrected signal yield is unfolded using the iterative D'Agostini method [42], as implemented in the RooUnfold software package [43], to take into account migrations between different bins due to the photon energy scale and resolution, and into and out of the fiducial E_T region. The

Table 2 Measured and predicted differential cross section for isolated-photon production, along with the statistical and systematical uncertainties in the various E_T and y bins. Predictions use JETPHOX at NLO with the NNPDF3.0 PDF set. The ratio of the JETPHOX predictions to data are listed in the last column, with the total uncertainty estimated assuming uncorrelated experimental and theoretical uncertainties

E_T (GeV)	Measured cross section within the bin (pb)	JETPHOX NNPDF3.0 (pb)	JETPHOX/Data
$\|y^\gamma\| < 0.8$			
190–200	$(3.64 \pm 0.04\,(\text{stat}) \pm 0.23\,(\text{syst})) \times 10^{-1}$	$(3.1 \pm 0.3) \times 10^{-1}$	0.85 ± 0.10
200–220	$(2.49 \pm 0.02\,(\text{stat}) \pm 0.15\,(\text{syst})) \times 10^{-1}$	$(2.2 \pm 0.2) \times 10^{-1}$	0.88 ± 0.09
220–250	$(1.46 \pm 0.01\,(\text{stat}) \pm 0.09\,(\text{syst})) \times 10^{-1}$	$(1.3 \pm 0.1) \times 10^{-1}$	0.90 ± 0.10
250–300	$(7.09 \pm 0.08\,(\text{stat}) \pm 0.45\,(\text{syst})) \times 10^{-2}$	$(6.4 \pm 0.5) \times 10^{-2}$	0.91 ± 0.10
300–350	$(2.91 \pm 0.05\,(\text{stat}) \pm 0.19\,(\text{syst})) \times 10^{-2}$	$(2.7 \pm 0.3) \times 10^{-2}$	0.92 ± 0.12
350–400	$(1.24 \pm 0.03\,(\text{stat}) \pm 0.10\,(\text{syst})) \times 10^{-2}$	$(1.4 \pm 0.2) \times 10^{-2}$	1.11 ± 0.15
400–500	$(5.1 \pm 0.1\,(\text{stat}) \pm 0.4\,(\text{syst})) \times 10^{-3}$	$(5.0 \pm 0.6) \times 10^{-3}$	0.98 ± 0.14
500–750	$(1.11 \pm 0.04\,(\text{stat}) \pm 0.08\,(\text{syst})) \times 10^{-3}$	$(9.0 \pm 1.0) \times 10^{-4}$	0.79 ± 0.14
750–1000	$(1.0 \pm 0.1\,(\text{stat}) \pm 0.1\,(\text{syst})) \times 10^{-4}$	$(1.4 \pm 0.4) \times 10^{-4}$	1.33 ± 0.44
$0.8 < \|y^\gamma\| < 1.44$			
190–200	$(3.44 \pm 0.04\,(\text{stat}) \pm 0.25\,(\text{syst})) \times 10^{-1}$	$(3.0 \pm 0.3) \times 10^{-1}$	0.88 ± 0.10
200–220	$(2.26 \pm 0.03\,(\text{stat}) \pm 0.18\,(\text{syst})) \times 10^{-1}$	$(2.1 \pm 0.2) \times 10^{-1}$	0.95 ± 0.12
220–250	$(1.37 \pm 0.02\,(\text{stat}) \pm 0.09\,(\text{syst})) \times 10^{-1}$	$(1.3 \pm 0.1) \times 10^{-1}$	0.94 ± 0.10
250–300	$(5.87 \pm 0.08\,(\text{stat}) \pm 0.40\,(\text{syst})) \times 10^{-2}$	$(6.2 \pm 0.6) \times 10^{-2}$	1.06 ± 0.12
300–350	$(2.60 \pm 0.05\,(\text{stat}) \pm 0.17\,(\text{syst})) \times 10^{-2}$	$(2.7 \pm 0.2) \times 10^{-2}$	1.04 ± 0.12
350–400	$(1.15 \pm 0.04\,(\text{stat}) \pm 0.09\,(\text{syst})) \times 10^{-2}$	$(1.3 \pm 0.1) \times 10^{-2}$	1.15 ± 0.13
400–500	$(4.6 \pm 0.2\,(\text{stat}) \pm 0.3\,(\text{syst})) \times 10^{-3}$	$(4.7 \pm 0.5) \times 10^{-3}$	1.04 ± 0.13
500–750	$(7.4 \pm 0.4\,(\text{stat}) \pm 0.6\,(\text{syst})) \times 10^{-4}$	$(8.2 \pm 0.8) \times 10^{-4}$	1.11 ± 0.15
750–1000	$(8.0 \pm 1.0\,(\text{stat}) \pm 1.0\,(\text{syst})) \times 10^{-5}$	$(1.1 \pm 0.2) \times 10^{-4}$	1.40 ± 0.39
$1.57 < \|y^\gamma\| < 2.1$			
190–200	$(3.16 \pm 0.05\,(\text{stat}) \pm 0.31\,(\text{syst})) \times 10^{-1}$	$(2.8 \pm 0.3) \times 10^{-1}$	0.88 ± 0.13
200–220	$(2.19 \pm 0.03\,(\text{stat}) \pm 0.19\,(\text{syst})) \times 10^{-1}$	$(2.0 \pm 0.2) \times 10^{-1}$	0.91 ± 0.12
220–250	$(1.19 \pm 0.02\,(\text{stat}) \pm 0.12\,(\text{syst})) \times 10^{-1}$	$(1.1 \pm 0.1) \times 10^{-1}$	0.96 ± 0.13
250–300	$(5.80 \pm 0.09\,(\text{stat}) \pm 0.54\,(\text{syst})) \times 10^{-2}$	$(5.4 \pm 0.5) \times 10^{-2}$	0.92 ± 0.12
300–350	$(2.37 \pm 0.06\,(\text{stat}) \pm 0.22\,(\text{syst})) \times 10^{-2}$	$(2.2 \pm 0.3) \times 10^{-2}$	0.93 ± 0.14
350–400	$(1.02 \pm 0.04\,(\text{stat}) \pm 0.12\,(\text{syst})) \times 10^{-2}$	$(9.5 \pm 0.9) \times 10^{-3}$	0.93 ± 0.15
400–500	$(4.0 \pm 0.2\,(\text{stat}) \pm 0.5\,(\text{syst})) \times 10^{-3}$	$(3.1 \pm 0.3) \times 10^{-3}$	0.77 ± 0.13
500–750	$(6.1 \pm 0.4\,(\text{stat}) \pm 0.9\,(\text{syst})) \times 10^{-4}$	$(4.6 \pm 0.5) \times 10^{-4}$	0.76 ± 0.14
750–1000	$(3.9 \pm 1.0\,(\text{stat}) \pm 1.1\,(\text{syst})) \times 10^{-5}$	$(3.0 \pm 0.9) \times 10^{-5}$	0.78 ± 0.37
$2.1 < \|y^\gamma\| < 2.5$			
190–200	$(2.52 \pm 0.07\,(\text{stat}) \pm 0.35\,(\text{syst})) \times 10^{-1}$	$(2.3 \pm 0.3) \times 10^{-1}$	0.92 ± 0.17
200–220	$(1.55 \pm 0.04\,(\text{stat}) \pm 0.14\,(\text{syst})) \times 10^{-1}$	$(1.6 \pm 0.2) \times 10^{-1}$	1.04 ± 0.14
220–250	$(8.8 \pm 0.2\,(\text{stat}) \pm 0.8\,(\text{syst})) \times 10^{-2}$	$(9.0 \pm 1.0) \times 10^{-2}$	1.02 ± 0.15
250–300	$(3.7 \pm 0.1\,(\text{stat}) \pm 0.4\,(\text{syst})) \times 10^{-2}$	$(3.8 \pm 0.4) \times 10^{-2}$	1.01 ± 0.14
300–350	$(1.32 \pm 0.07\,(\text{stat}) \pm 0.15\,(\text{syst})) \times 10^{-2}$	$(1.4 \pm 0.1) \times 10^{-2}$	1.06 ± 0.17
350–400	$(5.9 \pm 0.4\,(\text{stat}) \pm 0.7\,(\text{syst})) \times 10^{-3}$	$(5.0 \pm 0.5) \times 10^{-3}$	0.85 ± 0.14
400–500	$(1.7 \pm 0.1\,(\text{stat}) \pm 0.3\,(\text{syst})) \times 10^{-3}$	$(1.2 \pm 0.1) \times 10^{-3}$	0.72 ± 0.16
500–750	$(1.8 \pm 0.2\,(\text{stat}) \pm 0.4\,(\text{syst})) \times 10^{-4}$	$(1.4 \pm 0.3) \times 10^{-4}$	0.77 ± 0.25

unfolding response matrix is obtained from the PYTHIA 8 photon+jet sample. The unfolding corrections are small, of the order of 1%. The size of the corrections is also verified using an independent photon+jet sample generated with MADGRAPH.

The inclusive isolated-photon differential production cross section is calculated as

$$\frac{\mathrm{d}^2\sigma}{\mathrm{d}y^\gamma \mathrm{d}E_\mathrm{T}^\gamma} = \frac{\mathcal{U}(N^\gamma)}{\Delta y^\gamma\, \Delta E_\mathrm{T}^\gamma}\, \frac{1}{\epsilon\, \mathrm{SF}\, L}, \tag{1}$$

and the photon+jet as

$$\frac{\mathrm{d}^3\sigma}{\mathrm{d}y^\gamma \mathrm{d}E_\mathrm{T}^\gamma \mathrm{d}y^\mathrm{jet}} = \frac{\mathcal{U}(N^\gamma)}{\Delta y^\gamma\, \Delta E_\mathrm{T}^\gamma\, \Delta y^\mathrm{jet}}\, \frac{1}{\epsilon\, \mathrm{SF}\, L}, \tag{2}$$

where $\mathcal{U}(N^\gamma)$ denotes the unfolded photon yields in bins of width $\Delta E_\mathrm{T}^\gamma$ and Δy, and y is the rapidity of either the photon or the jet. In these equations, ϵ denotes the product of trigger, reconstruction, and selection efficiencies; SF the product of the selection and electron veto scale factors; and L is the integrated luminosity.

6 Systematic uncertainties

The uncertainty in the efficiency of the event selection is typically small except in the high-E_T region, where statistical uncertainties in both data and simulated events dominate. A summary of the systematic uncertainties in the cross section measurement, due to the uncertain in trigger and event selection efficiencies, Data-to-MC scale factors, signal and background template shapes, bin migrations from the unfolding procedure, and uncertainties in the photon energy scale and resolution, is given in Table 1. All of the above are treated as uncorrelated.

The systematic uncertainties in the trigger efficiency are dominated by the statistical uncertainty in jet trigger data where the trigger efficiencies are measured. The uncertainties of the selection efficiency are dominated by the statistical uncertainties of the simulation sample. The uncertainties of the Data-to-MC scale factor are based on the available Z → e$^+$e$^-$ events, and a p_T extrapolation is employed.

The systematic uncertainties in the signal and background templates are incorporated into the fit as nuisance parameters. For the signal template uncertainty, the nuisance parameter is assigned a Gaussian prior, while log-normal priors are assigned to the background template nuisances. A description of the general methodology can be found in Ref. [44]. The bias correction, applied to the photon yields, due to the selection of the sideband range is also considered as a systematic uncertainty.

The impact on photon yields due to the event migration between photon p_T bins from the unfolding uncertainties,
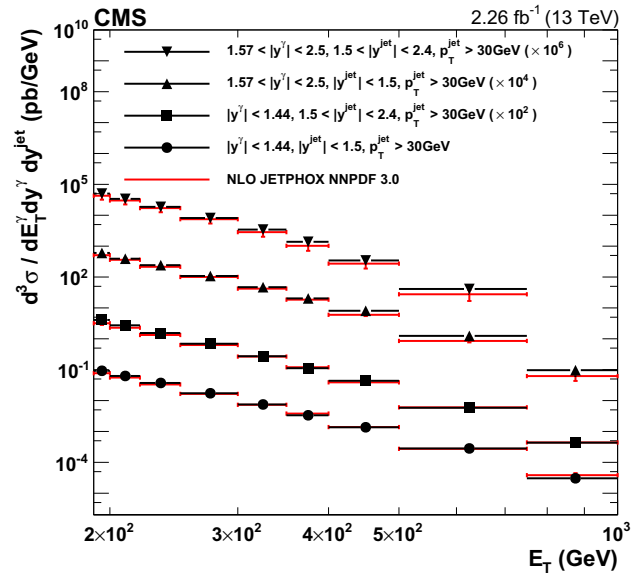

Fig. 5 Differential cross sections for photon+jet production in two photon rapidity bins, $|y^\gamma| < 1.44$ and $1.57 < |y^\gamma| < 2.5$, and two jet rapidity bins, $|y^\mathrm{jet}| < 1.5$ and $1.5 < |y^\mathrm{jet}| < 2.4$. The points show the measured values with their total uncertainties, and the lines show the NLO JETPHOX predictions with the NNPDF3.0 PDF set

which include photon energy scale and resolution uncertainties, is roughly 5%. The uncertainties of the event selection efficiency due to the jet selection, jet energy scale and resolution, and jet rapidity migration are negligible.

The total uncertainty, not considering luminosity uncertainty, in the yield per bin, excluding the highest photon E_T bin in each y range, is about 5–8% for EB and 9–17% for EE photons. The highest photon E_T bins in all y region have limited events in data and simulated samples for the evaluation of systematics.

The uncertainty in the measurement of the CMS integrated luminosity is 2.3% [22] and it is added in quadrature with other systematic uncertainties.

7 Results and comparison with theory

The measured inclusive isolated-photon cross sections as a function of photon E_T are shown in Fig. 3 and the ratio compared with theory in Fig. 4 for photon E_T greater than 190 GeV and $|y^\gamma| < 2.5$ in 4 rapidity bins. The results are listed in Table 2. The measurements for photon+jet cross sections as a function of photon E_T are shown in Fig. 5 and the ratio compared with theory in Fig. 6 with additional requirements of $p_\mathrm{T}^\mathrm{jet} > 30$ GeV and $|y^\mathrm{jet}| < 2.4$. The results are binned in two photon rapidity and two jet rapidity bins and are listed in Table 3. The predictions require an isolated photon at generator level as described previously, with a transverse isolation energy less than 5 GeV.
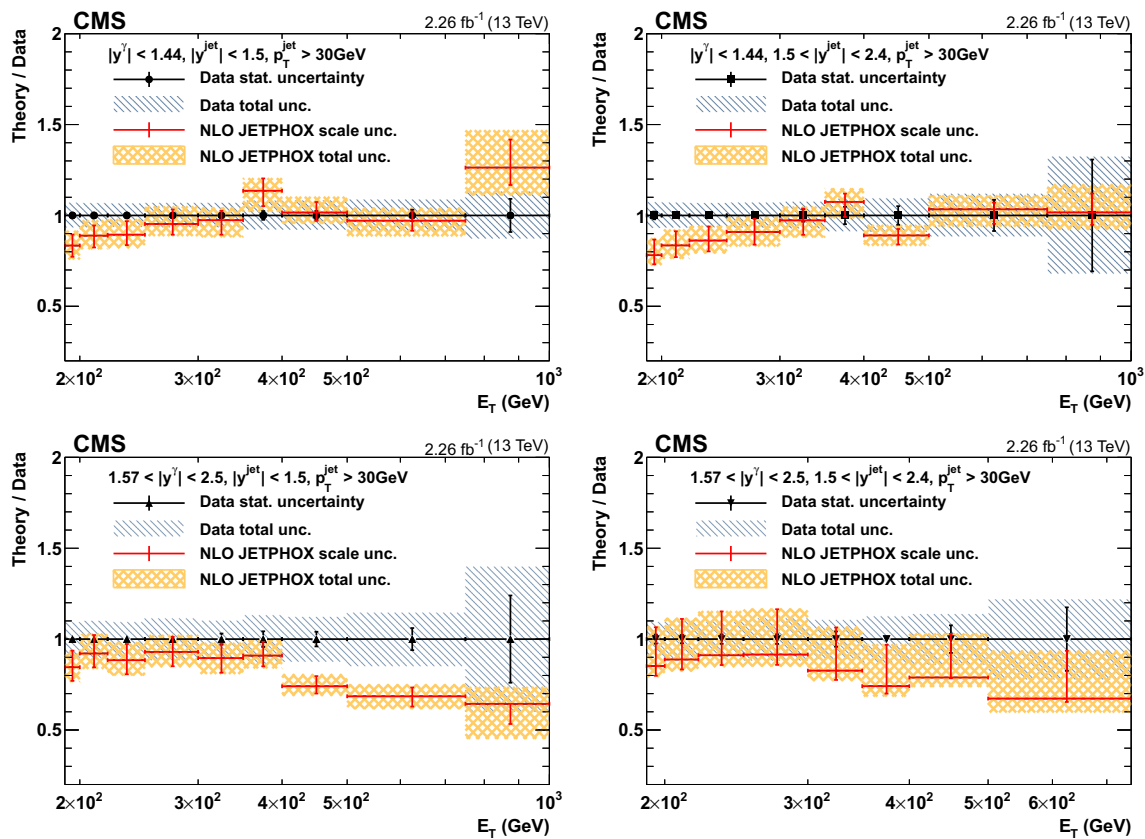
Fig. 6 The ratios of theoretical NLO prediction to data for the differential cross sections for photon+jet production in two photon rapidity ($|y^\gamma| < 1.44$ and $1.57 < |y^\gamma| < 2.5$) and two jet rapidity ($|y^{jet}| < 1.5$ and $1.5 < |y^{jet}| < 2.4$) bins , are shown. The error bars on the data points represent their statistical uncertainty, while the hatched area shows the total experimental uncertainty. The error bars on the ratios show the scale uncertainties, and the shaded area shows the total theoretical uncertainties

The measured cross sections in the overlapping photon ET regions are increased by approximately a factor of 3 to 5 compared to previous CMS measurements at 7 TeV [1,2,8]. This 13 TeV analysis also extends the photon E_T range from 400 (300) GeV in the 7 TeV inclusive photon (photon+jet) results to 1 TeV.

The measured cross sections are compared with NLO perturbative QCD calculations from the JETPHOX 1.3.1 generator [13,45,46], using the NNPDF3.0 NLO [18] PDFs and the Bourhis–Fontannaz–Guillet (BFG) set II parton fragmentation functions [47]. The renormalization, factorization, and fragmentation scales are all set to be equal to the photon E_T. To estimate the effect of the choice of theoretical scales on the predictions, the three scales are varied independently from $E_T/2$ to $2E_T$, while keeping their ratio between one-half and two. The impact of JETPHOX cross section predictions due to the uncertainties in the PDF and in the strong coupling $\alpha_S = 0.118$ at the mass of Z boson is calculated using the 68% confidence level NNPDF3.0 NLO replica. The uncertainty of parton-to-particle level transformation of the NLO pQCD prediction due to the underlying event and parton

shower is studied by comparing with dedicated PYTHIA samples where the choice and tuning of the generator has been modified. The differences between the dedicated PYTHIA and the nominal sample are between 0.5 and 2.0%, depending on the photon E_T and y, and they are assigned as the systematic uncertainty. The total theoretical uncertainties of the cross section predictions are evaluated as the quadratic sum of the scale, PDF, α_S, and underlying event and parton shower uncertainties.

The ratio of the theoretical predictions to data, together with the experimental and theoretical uncertainties, are shown in Figs. 4 and 6 for the isolated-photon and photon+jet cross section measurements respectively. The uncertainties in the theoretical predictions and ratios to data are symmetrized in the tables; the largest value between the positive and negative uncertainties is listed. Measured cross sections are in agreement with theoretical expectations within statistical and systematic uncertainties.

The ratio of the theoretical predictions to data based on JETPHOX at NLO with different PDF sets, including MMHT14 [19], CT14 [20], and HERAPDF2.0 [48] together

Table 3 Measured and predicted differential cross section for photon+jet production, along with statistical and systematical uncertainties in the various E_T and y bins. Predictions are based on JETPHOX at NLO with the NNPDF3.0 PDF set. The ratio of the JETPHOX predictions to the data are listed in the last column, with the total uncertainty estimated assuming uncorrelated experimental and theoretical uncertainties

| E_T (GeV)	Measured cross section within the bin (pb)	JETPHOX NNPDF3.0 (pb)	JETPHOX/Data
$\|y^\gamma\| < 1.44$, $\|y^{jet}\| < 1.5$, and $p_T^{jet} > 30\,\text{GeV}$			
190–200	$(9.2 \pm 0.1\,(\text{stat}) \pm 0.6\,(\text{syst})) \times 10^{-2}$	$(7.7 \pm 0.7) \times 10^{-2}$	0.83 ± 0.10
200–220	$(6.26 \pm 0.06\,(\text{stat}) \pm 0.41\,(\text{syst})) \times 10^{-2}$	$(5.6 \pm 0.5) \times 10^{-2}$	0.89 ± 0.10
220–250	$(3.72 \pm 0.04\,(\text{stat}) \pm 0.23\,(\text{syst})) \times 10^{-2}$	$(3.3 \pm 0.3) \times 10^{-2}$	0.89 ± 0.10
250–300	$(1.72 \pm 0.02\,(\text{stat}) \pm 0.11\,(\text{syst})) \times 10^{-2}$	$(1.6 \pm 0.2) \times 10^{-2}$	0.95 ± 0.12
300–350	$(7.50 \pm 0.1\,(\text{stat}) \pm 0.5\,(\text{syst})) \times 10^{-3}$	$(7.3 \pm 0.7) \times 10^{-3}$	0.97 ± 0.11
350–400	$(3.34 \pm 0.08\,(\text{stat}) \pm 0.25\,(\text{syst})) \times 10^{-3}$	$(3.8 \pm 0.4) \times 10^{-3}$	1.14 ± 0.15
400–500	$(1.37 \pm 0.03\,(\text{stat}) \pm 0.10\,(\text{syst})) \times 10^{-3}$	$(1.4 \pm 0.1) \times 10^{-3}$	1.02 ± 0.12
500–750	$(2.82 \pm 0.09\,(\text{stat}) \pm 0.22\,(\text{syst})) \times 10^{-4}$	$(2.7 \pm 0.2) \times 10^{-4}$	0.97 ± 0.12
750–1000	$(3.0 \pm 0.3\,(\text{stat}) \pm 0.3\,(\text{syst})) \times 10^{-5}$	$(3.8 \pm 0.6) \times 10^{-5}$	1.26 ± 0.26
$\|y^\gamma\| < 1.44$, $1.5 < \|y^{jet}\| < 2.4$, and $p_T^{jet} > 30\,\text{GeV}$			
190–200	$(4.08 \pm 0.09\,(\text{stat}) \pm 0.27\,(\text{syst})) \times 10^{-2}$	$(3.2 \pm 0.4) \times 10^{-2}$	0.78 ± 0.11
200–220	$(2.73 \pm 0.05\,(\text{stat}) \pm 0.18\,(\text{syst})) \times 10^{-2}$	$(2.3 \pm 0.2) \times 10^{-2}$	0.84 ± 0.10
220–250	$(1.54 \pm 0.03\,(\text{stat}) \pm 0.10\,(\text{syst})) \times 10^{-2}$	$(1.3 \pm 0.1) \times 10^{-2}$	0.86 ± 0.10
250–300	$(6.9 \pm 0.1\,(\text{stat}) \pm 0.5\,(\text{syst})) \times 10^{-3}$	$(6.3 \pm 0.6) \times 10^{-3}$	0.91 ± 0.10
300–350	$(2.73 \pm 0.09\,(\text{stat}) \pm 0.18\,(\text{syst})) \times 10^{-3}$	$(2.7 \pm 0.3) \times 10^{-3}$	0.97 ± 0.12
350–400	$(1.12 \pm 0.05\,(\text{stat}) \pm 0.08\,(\text{syst})) \times 10^{-3}$	$(1.2 \pm 0.1) \times 10^{-3}$	1.07 ± 0.13
400–500	$(4.4 \pm 0.2\,(\text{stat}) \pm 0.3\,(\text{syst})) \times 10^{-4}$	$(3.9 \pm 0.3) \times 10^{-4}$	0.89 ± 0.10
500–750	$(5.8 \pm 0.5\,(\text{stat}) \pm 0.5\,(\text{syst})) \times 10^{-5}$	$(6.0 \pm 0.6) \times 10^{-5}$	1.03 ± 0.15
750–1000	$(4.3 \pm 1.3\,(\text{stat}) \pm 0.4\,(\text{syst})) \times 10^{-6}$	$(4.4 \pm 0.7) \times 10^{-6}$	1.02 ± 0.36
$1.57 < \|y^\gamma\| < 2.5$, $\|y^{jet}\| < 1.5$, and $p_T^{jet} > 30\,\text{GeV}$			
190–200	$(6.0 \pm 0.1\,(\text{stat}) \pm 0.6\,(\text{syst})) \times 10^{-2}$	$(5.1 \pm 0.6) \times 10^{-2}$	0.85 ± 0.12
200–220	$(3.92 \pm 0.08\,(\text{stat}) \pm 0.39\,(\text{syst})) \times 10^{-2}$	$(3.6 \pm 0.4) \times 10^{-2}$	0.92 ± 0.14
220–250	$(2.42 \pm 0.04\,(\text{stat}) \pm 0.23\,(\text{syst})) \times 10^{-2}$	$(2.1 \pm 0.2) \times 10^{-2}$	0.88 ± 0.13
250–300	$(1.08 \pm 0.02\,(\text{stat}) \pm 0.12\,(\text{syst})) \times 10^{-2}$	$(1.0 \pm 0.1) \times 10^{-2}$	0.93 ± 0.14
300–350	$(4.7 \pm 0.1\,(\text{stat}) \pm 0.5\,(\text{syst})) \times 10^{-3}$	$(4.2 \pm 0.4) \times 10^{-3}$	0.90 ± 0.13
350–400	$(2.03 \pm 0.09\,(\text{stat}) \pm 0.25\,(\text{syst})) \times 10^{-3}$	$(1.8 \pm 0.2) \times 10^{-3}$	0.91 ± 0.15
400–500	$(8.1 \pm 0.3\,(\text{stat}) \pm 0.9\,(\text{syst})) \times 10^{-4}$	$(6.0 \pm 0.5) \times 10^{-4}$	0.74 ± 0.11
500–750	$(1.24 \pm 0.08\,(\text{stat}) \pm 0.17\,(\text{syst})) \times 10^{-4}$	$(8.5 \pm 0.9) \times 10^{-5}$	0.69 ± 0.12
750–1000	$(1.0 \pm 0.2\,(\text{stat}) \pm 0.3\,(\text{syst})) \times 10^{-5}$	$(6.0 \pm 2.0) \times 10^{-6}$	0.64 ± 0.32
$1.57 < \|y^\gamma\| < 2.5$, $1.5 < \|y^{jet}\| < 2.4$, and $p_T^{jet} > 30\,\text{GeV}$			
190–200	$(5.0 \pm 0.1\,(\text{stat}) \pm 0.5\,(\text{syst})) \times 10^{-2}$	$(4.0 \pm 1.0) \times 10^{-2}$	0.85 ± 0.23
200–220	$(3.39 \pm 0.08\,(\text{stat}) \pm 0.34\,(\text{syst})) \times 10^{-2}$	$(3.0 \pm 0.8) \times 10^{-2}$	0.89 ± 0.24
220–250	$(1.87 \pm 0.05\,(\text{stat}) \pm 0.17\,(\text{syst})) \times 10^{-2}$	$(1.7 \pm 0.5) \times 10^{-2}$	0.91 ± 0.26
250–300	$(8.1 \pm 0.2\,(\text{stat}) \pm 0.9\,(\text{syst})) \times 10^{-3}$	$(7.0 \pm 2.0) \times 10^{-3}$	0.92 ± 0.27
300–350	$(3.4 \pm 0.1\,(\text{stat}) \pm 0.3\,(\text{syst})) \times 10^{-3}$	$(2.8 \pm 0.8) \times 10^{-3}$	0.83 ± 0.26
350–400	$(1.38 \pm 0.02\,(\text{stat}) \pm 0.17\,(\text{syst})) \times 10^{-3}$	$(1.0 \pm 0.3) \times 10^{-3}$	0.74 ± 0.25
400–500	$(3.4 \pm 0.3\,(\text{stat}) \pm 0.4\,(\text{syst})) \times 10^{-4}$	$(2.7 \pm 0.8) \times 10^{-4}$	0.79 ± 0.27
500–750	$(4.1 \pm 0.7\,(\text{stat}) \pm 0.5\,(\text{syst})) \times 10^{-5}$	$(3.0 \pm 1.0) \times 10^{-5}$	0.67 ± 0.30
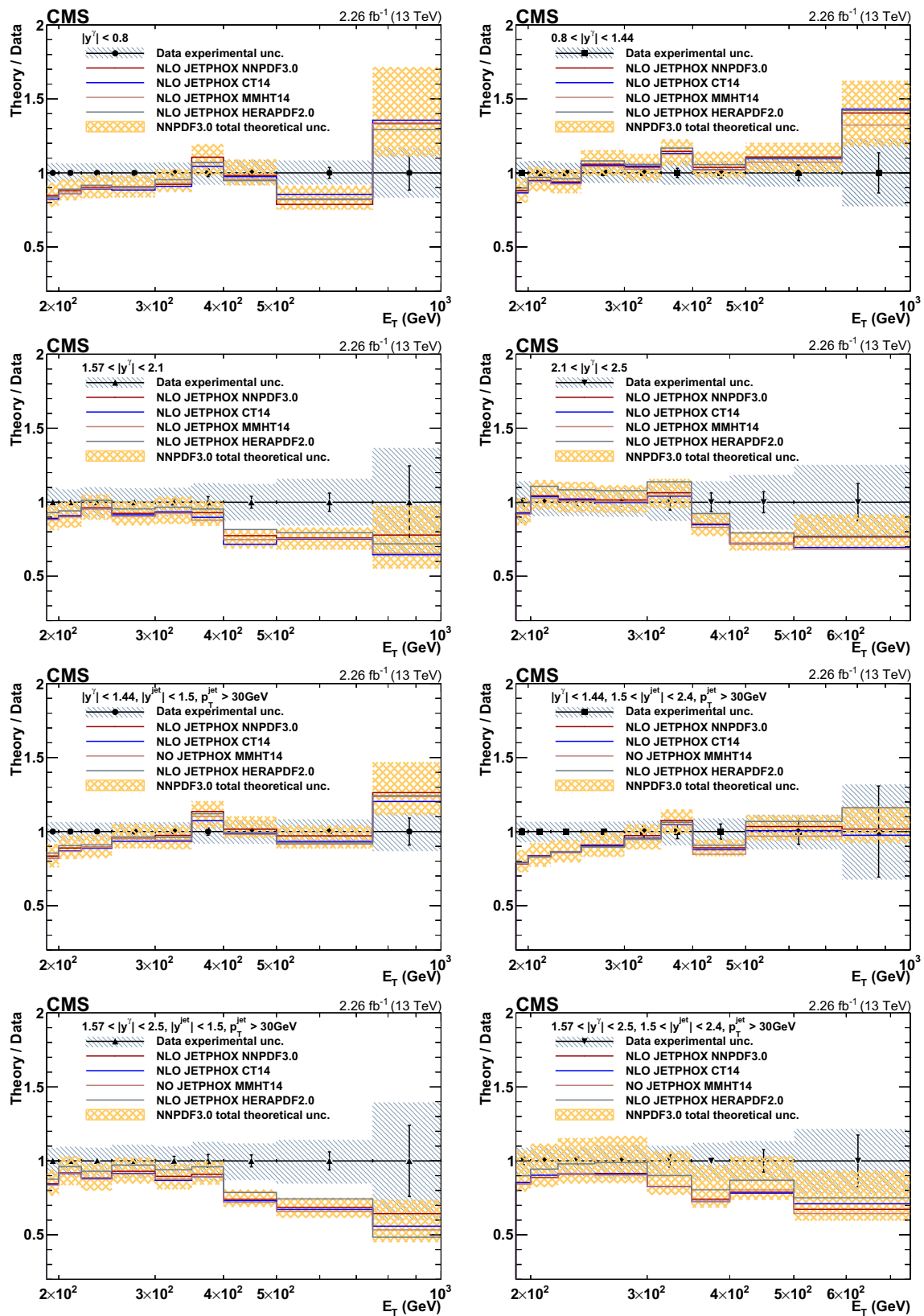
Fig. 7 Ratios of JETPHOX NLO predictions to data for various PDF sets as a function of photon E_T for inclusive isolated-photons (top four panels) and photon+jet (four bottom panels). Data are shown as points, the error bars represent statistical uncertainties, while the hatched area represents the total experimental uncertainties. The theoretical uncertainty in the NNPDF3.0 prediction is shown as a shaded area

with NNPDF3.0, are shown in Fig. 7. The differences between JETPHOX predictions using different PDF sets are small, within the theoretical uncertainties estimated with NNPDF3.0.

8 Summary

The differential cross sections for inclusive isolated-photon and photon+jet production in proton-proton collisions at a center-of-mass energy of 13 TeV are measured with a data sample collected by the CMS experiment corresponding to an integrated luminosity of 2.26 fb^{-1}. The measurements of inclusive isolated-photon production cross sections are presented as functions of photon transverse energy and rapidity with $E_T^\gamma > 190$ GeV and $|y^\gamma| < 2.5$. The photon+jet production cross sections are presented as functions of photon transverse energy, and photon and jet rapidities, with requirement of an isolated photon and jet where $p_T^{jet} > 30$ GeV and $|y^{jet}| < 2.4$.

The measurements are compared with theoretical predictions produced using the JETPHOX next-to-leading order calculations using different parton distribution functions. The theoretical predictions agree with the experimental measurements within the statistical and systematic uncertainties. For low to middle range in photon E_T, where the experimental uncertainties are smaller or comparable to theoretical uncertainties, these measurements provide the potential to further constrain the proton PDFs. The agreement between data and theory, and the new next-to-next-to-leading-order (NNLO) calculations [49] motivate the use of additional measurements to better estimate the gluon and other PDFs.

References

1. CMS Collaboration, Measurement of the isolated prompt photon production cross section in pp collisions at $\sqrt{s} = 7$ TeV. Phys. Rev. Lett. 106, 082001 (2011). doi: 10.1103/PhysRevLett. 106.082001. arXiv:1012.0799

2. CMS Collaboration, Measurement of the differential cross section for isolated prompt photon production in pp collisions at 7 TeV. Phys. Rev. D **84**, 052011 (2011). https://doi.org/10.1103/PhysRevD.84.052011. arXiv:1108.2044

3. CMS Collaboration, Measurement of isolated photon production in pp and PbPb collisions at $\sqrt{s_{NN}} = 2.76$ TeV. Phys. Lett. B **710**, 256 (2012). https://doi.org/10.1016/j.physletb.2012.02.077. arXiv:1201.3093

4. ATLAS Collaboration, Measurement of the inclusive isolated prompt photon cross section in pp collisions at $\sqrt{s} = 7$ TeV with the ATLAS detector. Phys. Rev. D **83**, 052005 (2011). https://doi.org/10.1103/PhysRevD.83.052005. arXiv:1012.4389

5. ATLAS Collaboration, Measurement of the inclusive isolated prompt photon cross-section in pp collisions at $\sqrt{s} = 7$ TeV using 35 pb^{-1} of ATLAS data. Phys. Lett. B **706**, 150 (2011). https://doi.org/10.1016/j.physletb.2011.11.010. arXiv:1108.0253

6. ATLAS Collaboration, Measurement of the inclusive isolated prompt photons cross section in pp collisions at $\sqrt{s} = 7$

TeV with the ATLAS detector using $4.6\,\text{fb}^{-1}$. Phys. Rev. D **89**, 052004 (2014). https://doi.org/10.1103/PhysRevD.89.052004. arXiv:1311.1440

7. ATLAS Collaboration, Measurement of the inclusive isolated prompt photon cross section in pp collisions at $\sqrt{s} = 8$ TeV with the ATLAS detector. JHEP **08**, 005 (2016). https://doi.org/10.1007/JHEP08(2016)005. arXiv:1605.03495

8. CMS Collaboration, Measurement of the triple-differential cross section for photon+jets production in proton-proton collisions at $\sqrt{s} = 7$ TeV. JHEP **06**, 009 (2014). https://doi.org/10.1007/JHEP06(2014)009. arXiv:1311.6141

9. ATLAS Collaboration, Measurement of the production cross section of an isolated photon associated with jets in proton-proton collisions at $\sqrt{s} = 7$ TeV with the ATLAS detector. Phys. Rev. D **85**, 092014 (2012). https://doi.org/10.1103/PhysRevD.85.092014. arXiv:1203.3161

10. ATLAS Collaboration, High-E_T isolated-photon plus jets production in pp collisions at $\sqrt{s} = 8$ TeV with the ATLAS detector. Nucl. Phys. B **918**, 257 (2017). https://doi.org/10.1016/j.nuclphysb.2017.03.006. arXiv:1611.06586

11. ATLAS Collaboration, Measurement of the cross section for inclusive isolated-photon production in pp collisions at $\sqrt{s} = 13$ TeV using the ATLAS detector. Phys. Lett. B **770**, 473 (2017). https://doi.org/10.1016/j.physletb.2017.04.072. arXiv:1701.06882

12. ATLAS Collaboration, Measurement of the cross section for isolated-photon plus jet production in pp collisions at $\sqrt{s} = 13$ TeV using the ATLAS detector. Phys. Lett. B **780**, 578 (2018). https://doi.org/10.1016/j.physletb.2018.03.035. arXiv:1801.00112

13. P. Aurenche et al., A new critical study of photon production in hadronic collisions. Phys. Rev. D **73**, 094007 (2006). https://doi.org/10.1103/PhysRevD.73.094007. arXiv:hep-ph/0602133

14. R. Ichou, D. d'Enterria, Sensitivity of isolated photon production at TeV hadron colliders to the gluon distribution in the proton. Phys. Rev. D **82**, 014015 (2010). https://doi.org/10.1103/PhysRevD.82.014015. arXiv:1005.4529

15. W. Vogelsang, A. Vogt, Constraints on the proton's gluon distribution from prompt photon production. Nucl. Phys. B **453**, 334 (1995). https://doi.org/10.1016/0550-3213(95)00424-Q. arXiv:hep-ph/9505404

16. D. d'Enterria, J. Rojo, Quantitative constraints on the gluon distribution function in the proton from collider isolated-photon data. Nucl. Phys. B **860**, 311 (2012). https://doi.org/10.1016/j.nuclphysb.2012.03.003. arXiv:1202.1762

17. L. Carminati et al., Sensitivity of the LHC isolated-gamma+jet data to the parton distribution functions of the proton. EPL **101**, 61002 (2013). https://doi.org/10.1209/0295-5075/101/61002. arXiv:1212.5511

18. NNPDF Collaboration, Parton distributions for the LHC Run II. JHEP **04**, 040 (2015). https://doi.org/10.1007/JHEP04(2015)040. arXiv:1410.8849

19. L.A. Harland-Lang, A.D. Martin, P. Motylinski, R.S. Thorne, Parton distributions in the LHC era: MMHT 2014 PDFs. Eur. Phys. J. C **75**, 204 (2015). https://doi.org/10.1140/epjc/s10052-015-3397-6. arXiv:1412.3989

20. S. Dulat et al., New parton distribution functions from a global analysis of quantum chromodynamics. Phys. Rev. D **93**, 033006 (2016). https://doi.org/10.1103/PhysRevD.93.033006. arXiv:1506.07443

21. J.M. Campbell, J. Rojo, E. Slade, C. Williams, Direct photon production and PDF fits reloaded. Eur. Phys. J. C **78**, 470 (2018). https://doi.org/10.1140/epjc/s10052-018-5944-4. arXiv:1802.03021

22. CMS Collaboration, CMS luminosity measurement for the 2015 data-taking period. CMS Physics Analysis Summary CMS-PAS-LUM-15-001 (2016). https://cds.cern.ch/record/2138682

23. H. Voss, A. Höcker, J. Stelzer, F. Tegenfeldt, TMVA, the toolkit for multivariate data analysis with ROOT. In *XIth International Workshop on Advanced Computing and Analysis Techniques in Physics Research (ACAT)*, (2007). p. 40. arXiv:physics/0703039. https://doi.org/10.22323/1.050.0040

24. CMS Collaboration, The CMS Experiment at the CERN LHC. JINST **3**, S08004 (2008). https://doi.org/10.1088/1748-0221/3/08/S08004

25. CMS Collaboration, Description and performance of track and primary-vertex reconstruction with the CMS tracker. JINST **9**, P10009 (2014). https://doi.org/10.1088/1748-0221/9/10/P10009. arXiv:1405.6569

26. CMS Collaboration, Particle-flow reconstruction and global event description with the CMS detector. JINST **12**, P10003 (2017). https://doi.org/10.1088/1748-0221/12/10/P10003. arXiv:1706.04965

27. CMS Collaboration, Energy calibration and resolution of the CMS electromagnetic calorimeter in pp collisions at $\sqrt{s} = 7$ TeV. JINST **8**, P09009 (2013). https://doi.org/10.1088/1748-0221/8/09/P09009. arXiv:1306.2016

28. CMS Collaboration, Performance of photon reconstruction and identification with the CMS detector in proton-proton collisions at $\sqrt{s} = 8$ TeV. JINST **10**, P08010 (2015). https://doi.org/10.1088/1748-0221/10/08/P08010. arXiv:1502.02702

29. M. Cacciari, G.P. Salam, G. Soyez, The anti-k_T jet clustering algorithm. JHEP **04**, 063 (2008). https://doi.org/10.1088/1126-6708/2008/04/063. arXiv:0802.1189

30. M. Cacciari, G.P. Salam, G. Soyez, FastJet user manual. Eur. Phys. J. C **72**, 1896 (2012). https://doi.org/10.1140/epjc/s10052-012-1896-2. arXiv:1111.6097

31. CMS Collaboration, Jet energy scale and resolution in the CMS experiment in pp collisions at 8 TeV. JINST **12**, P02014 (2017). https://doi.org/10.1088/1748-0221/12/02/P02014. arXiv:1607.03663

32. T. Sjöstrand et al., An Introduction to PYTHIA 8.2. Comput. Phys. Commun. **191**, 159 (2015). https://doi.org/10.1016/j.cpc.2015.01.024. arXiv:1410.3012

33. J. Alwall et al., The automated computation of tree-level and next-to-leading order differential cross sections, and their matching to parton shower simulations. JHEP **07**, 079 (2014). https://doi.org/10.1007/JHEP07(2014)079. arXiv:1405.0301

34. J. Alwall et al., Comparative study of various algorithms for the merging of parton showers and matrix elements in hadronic collisions. Eur. Phys. J. C **53**, 473 (2008). https://doi.org/10.1140/epjc/s10052-007-0490-5. arXiv:0706.2569

35. R. Frederix, S. Frixione, Merging meets matching in MC@NLO. JHEP **12**, 061 (2012). https://doi.org/10.1007/JHEP12(2012)061. arXiv:1209.6215

36. CMS Collaboration, Event generator tunes obtained from underlying event and multiparton scattering measurements. Eur. Phys. J. C **76**, 155 (2016). https://doi.org/10.1140/epjc/s10052-016-3988-x. arXiv:1512.00815

37. NNPDF Collaboration, Parton distributions with LHC data. Nucl. Phys. B **867**, 244 (2013). https://doi.org/10.1016/j.nuclphysb.2012.10.003. arXiv:1207.1303

38. GEANT4 Collaboration, GEANT4—a simulation toolkit. Nucl. Instrum. Methods A **506**, 250 (2003). https://doi.org/10.1016/S0168-9002(03)01368-8

39. CMS Collaboration, The CMS trigger system. JINST **12**, P01020 (2017). https://doi.org/10.1088/1748-0221/12/01/P01020. arXiv:1609.02366

40. CMS Collaboration, Performance of missing energy reconstruction in 13 TeV pp collision data using the CMS detector. CMS Physics Analysis Summary CMS-PAS-JME-16-004 (2016). https://cds.cern.ch/record/2205284

41. CMS Collaboration, Jet algorithms performance in 13 TeV data. CMS Physics Analysis Summary CMS-PAS-JME-16-003 (2017). https://cds.cern.ch/record/2256875

43. T. Adye, Unfolding algorithms and tests using RooUnfold. Proceedings, PHYSTAT 2011 Workshop on Statistical Issues Related to Discovery Claims in Search Experiments and Unfolding **313**, (2011). https://doi.org/10.5170/CERN-2011-006.313. arXiv:1105.1160

44. ATLAS and CMS Collaborations, LHC Higgs Combination Group, Procedure for the LHC Higgs boson search combination in summer 2011. CMS/ATLAS joint note ATL-PHYS-PUB-2011-11, CMS NOTE 2011/005 (2011)

45. S. Catani, M. Fontannaz, J.P. Guillet, E. Pilon, Cross section of isolated prompt photons in hadron–hadron collisions. JHEP **05**, 028 (2002). https://doi.org/10.1088/1126-6708/2002/05/028. arXiv:hep-ph/0204023

46. Z. Belghobsi et al., Photon-jet correlations and constraints on fragmentation functions. Phys. Rev. D **79**, 114024 (2009). https://doi.org/10.1103/PhysRevD.79.114024. arXiv:0903.4834

47. L. Bourhis, M. Fontannaz, J.P. Guillet, Quark and gluon fragmentation functions into photons. Eur. Phys. J. C **2**, 529 (1998). https://doi.org/10.1007/s100520050158. arXiv:hep-ph/9704447

48. H1 and ZEUS Collaborations, Combination of measurements of inclusive deep inelastic $e^{\pm}p$ scattering cross sections and QCD analysis of HERA data. Eur. Phys. J. C **75**, 580 (2015). https://doi.org/10.1140/epjc/s10052-015-3710-4. arXiv:1506.06042

49. J.M. Campbell, R.K. Ellis, C. Williams, Direct photon production at next-to-next-to-leading order. Phys. Rev. Lett. **118**, 222001 (2017). https://doi.org/10.1103/PhysRevLett.118.222001. arXiv:1612.04333

CMS Collaboration

Yerevan Physics Institute, Yerevan, Armenia
A. M. Sirunyan, A. Tumasyan

Institut für Hochenergiephysik, Wien, Austria
W. Adam, F. Ambrogi, E. Asilar, T. Bergauer, J. Brandstetter, E. Brondolin, M. Dragicevic, J. Erö, A. Escalante Del Valle, M. Flechl, R. Frühwirth[1], V. M. Ghete, J. Hrubec, M. Jeitler[1], N. Krammer, I. Krätschmer, D. Liko, T. Madlener, I. Mikulec, N. Rad, H. Rohringer, J. Schieck[1], R. Schöfbeck, M. Spanring, D. Spitzbart, A. Taurok, W. Waltenberger, J. Wittmann, C.-E. Wulz[1], M. Zarucki

Institute for Nuclear Problems, Minsk, Belarus
V. Chekhovsky, V. Mossolov, J. Suarez Gonzalez

Universiteit Antwerpen, Antwerpen, Belgium
E. A. De Wolf, D. Di Croce, X. Janssen, J. Lauwers, M. Pieters, M. Van De Klundert, H. Van Haevermaet, P. Van Mechelen, N. Van Remortel

Vrije Universiteit Brussel, Brussel, Belgium
S. Abu Zeid, F. Blekman, J. D'Hondt, I. De Bruyn, J. De Clercq, K. Deroover, G. Flouris, D. Lontkovskyi, S. Lowette, I. Marchesini, S. Moortgat, L. Moreels, Q. Python, K. Skovpen, S. Tavernier, W. Van Doninck, P. Van Mulders, I. Van Parijs

Université Libre de Bruxelles, Bruxelles, Belgium
D. Beghin, B. Bilin, H. Brun, B. Clerbaux, G. De Lentdecker, H. Delannoy, B. Dorney, G. Fasanella, L. Favart, R. Goldouzian, A. Grebenyuk, A. K. Kalsi, T. Lenzi, J. Luetic, N. Postiau, E. Starling, L. Thomas, C. Vander Velde, P. Vanlaer, D. Vannerom, Q. Wang

Ghent University, Ghent, Belgium
T. Cornelis, D. Dobur, A. Fagot, M. Gul, I. Khvastunov[2], D. Poyraz, C. Roskas, D. Trocino, M. Tytgat, W. Verbeke, B. Vermassen, M. Vit, N. Zaganidis

Université Catholique de Louvain, Louvain-la-Neuve, Belgium
H. Bakhshiansohi, O. Bondu, S. Brochet, G. Bruno, C. Caputo, P. David, C. Delaere, M. Delcourt, B. Francois, A. Giammanco, G. Krintiras, V. Lemaitre, A. Magitteri, A. Mertens, M. Musich, K. Piotrzkowski, A. Saggio, M. Vidal Marono, S. Wertz, J. Zobec

Centro Brasileiro de Pesquisas Fisicas, Rio de Janeiro, Brazil
F. L. Alves, G. A. Alves, L. Brito, G. Correia Silva, C. Hensel, A. Moraes, M. E. Pol, P. Rebello Teles

Universidade do Estado do Rio de Janeiro, Rio de Janeiro, Brazil
E. Belchior Batista Das Chagas, W. Carvalho, J. Chinellato[3], E. Coelho, E. M. Da Costa, G. G. Da Silveira[4], D. De Jesus Damiao, C. De Oliveira Martins, S. Fonseca De Souza, H. Malbouisson, D. Matos Figueiredo, M. Melo De Almeida, C. Mora Herrera, L. Mundim, H. Nogima, W. L. Prado Da Silva, L. J. Sanchez Rosas, A. Santoro, A. Sznajder, M. Thiel, E. J. Tonelli Manganote[3], F. Torres Da Silva De Araujo, A. Vilela Pereira

Universidade Estadual Paulista[a], Universidade Federal do ABC[b], São Paulo, Brazil
S. Ahuja[a], C. A. Bernardes[a], L. Calligaris[a], T. R. Fernandez Perez Tomei[a], E. M. Gregores[b], P. G. Mercadante[b], S. F. Novaes[a], Sandra S. Padula[a], D. Romero Abad[b]

Institute for Nuclear Research and Nuclear Energy, Bulgarian Academy of Sciences, Sofia, Bulgaria
A. Aleksandrov, R. Hadjiiska, P. Iaydjiev, A. Marinov, M. Misheva, M. Rodozov, M. Shopova, G. Sultanov

University of Sofia, Sofia, Bulgaria
A. Dimitrov, L. Litov, B. Pavlov, P. Petkov

Beihang University, Beijing, China
W. Fang[5], X. Gao[5], L. Yuan

Institute of High Energy Physics, Beijing, China
M. Ahmad, J. G. Bian, G. M. Chen, H. S. Chen, M. Chen, Y. Chen, C. H. Jiang, D. Leggat, H. Liao, Z. Liu, F. Romeo, S. M. Shaheen, A. Spiezia, J. Tao, C. Wang, Z. Wang, E. Yazgan, H. Zhang, J. Zhao

State Key Laboratory of Nuclear Physics and Technology, Peking University, Beijing, China
Y. Ban, G. Chen, A. Levin, J. Li, L. Li, Q. Li, Y. Mao, S. J. Qian, D. Wang, Z. Xu

Tsinghua University, Beijing, China
Y. Wang

Universidad de Los Andes, Bogota, Colombia
C. Avila, A. Cabrera, C. A. Carrillo Montoya, L. F. Chaparro Sierra, C. Florez, C. F. González Hernández, M. A. Segura Delgado

University of Split, Faculty of Electrical Engineering, Mechanical Engineering and Naval Architecture, Split, Croatia
B. Courbon, N. Godinovic, D. Lelas, I. Puljak, T. Sculac

University of Split, Faculty of Science, Split, Croatia
Z. Antunovic, M. Kovac

Institute Rudjer Boskovic, Zagreb, Croatia
V. Brigljevic, D. Ferencek, K. Kadija, B. Mesic, A. Starodumov[6], T. Susa

University of Cyprus, Nicosia, Cyprus
M. W. Ather, A. Attikis, M. Kolosova, G. Mavromanolakis, J. Mousa, C. Nicolaou, F. Ptochos, P. A. Razis, H. Rykaczewski

Charles University, Prague, Czech Republic
M. Finger[7], M. Finger Jr.[7]

Escuela Politecnica Nacional, Quito, Ecuador
E. Ayala

Universidad San Francisco de Quito, Quito, Ecuador
E. Carrera Jarrin

Academy of Scientific Research and Technology of the Arab Republic of Egypt, Egyptian Network of High Energy Physics, Cairo, Egypt
A. Ellithi Kamel[8], M. A. Mahmoud[9,10], E. Salama[10,11]

National Institute of Chemical Physics and Biophysics, Tallinn, Estonia
S. Bhowmik, A. Carvalho Antunes De Oliveira, R. K. Dewanjee, K. Ehataht, M. Kadastik, M. Raidal, C. Veelken

Department of Physics, University of Helsinki, Helsinki, Finland
P. Eerola, H. Kirschenmann, J. Pekkanen, M. Voutilainen

Helsinki Institute of Physics, Helsinki, Finland

J. Havukainen, J. K. Heikkilä, T. Järvinen, V. Karimäki, R. Kinnunen, T. Lampén, K. Lassila-Perini, S. Laurila, S. Lehti, T. Lindén, P. Luukka, T. Mäenpää, H. Siikonen, E. Tuominen, J. Tuominiemi

Lappeenranta University of Technology, Lappeenranta, Finland

T. Tuuva

IRFU, CEA, Université Paris-Saclay, Gif-sur-Yvette, France

M. Besancon, F. Couderc, M. Dejardin, D. Denegri, J. L. Faure, F. Ferri, S. Ganjour, A. Givernaud, P. Gras, G. Hamel de Monchenault, P. Jarry, C. Leloup, E. Locci, J. Malcles, G. Negro, J. Rander, A. Rosowsky, M. Ö. Sahin, M. Titov

Laboratoire Leprince-Ringuet, Ecole polytechnique, CNRS/IN2P3, Université Paris-Saclay, Palaiseau, France

A. Abdulsalam[12], C. Amendola, I. Antropov, F. Beaudette, P. Busson, C. Charlot, R. Granier de Cassagnac, I. Kucher, S. Lisniak, A. Lobanov, J. Martin Blanco, M. Nguyen, C. Ochando, G. Ortona, P. Pigard, R. Salerno, J. B. Sauvan, Y. Sirois, A. G. Stahl Leiton, A. Zabi, A. Zghiche

Université de Strasbourg, CNRS, IPHC UMR 7178, 67000 Strasbourg, France

J.-L. Agram[13], J. Andrea, D. Bloch, J.-M. Brom, E. C. Chabert, V Cherepanov, C. Collard, E. Conte[13], J.-C. Fontaine[13], D. Gelé, U. Goerlach, M. Jansová, A.-C. Le Bihan, N. Tonon, P. Van Hove

Centre de Calcul de l'Institut National de Physique Nucleaire et de Physique des Particules, CNRS/IN2P3, Villeurbanne, France

S. Gadrat

Université de Lyon, Université Claude Bernard Lyon 1, CNRS-IN2P3, Institut de Physique Nucléaire de Lyon, Villeurbanne, France

S. Beauceron, C. Bernet, G. Boudoul, N. Chanon, R. Chierici, D. Contardo, P. Depasse, H. El Mamouni, J. Fay, L. Finco, S. Gascon, M. Gouzevitch, G. Grenier, B. Ille, F. Lagarde, I. B. Laktineh, H. Lattaud, M. Lethuillier, L. Mirabito, A. L. Pequegnot, S. Perries, A. Popov[14], V. Sordini, M. Vander Donckt, S. Viret, S. Zhang

Georgian Technical University, Tbilisi, Georgia

T. Toriashvili[15]

Tbilisi State University, Tbilisi, Georgia

Z. Tsamalaidze[7]

RWTH Aachen University, I. Physikalisches Institut, Aachen, Germany

C. Autermann, L. Feld, M. K. Kiesel, K. Klein, M. Lipinski, M. Preuten, M. P. Rauch, C. Schomakers, J. Schulz, M. Teroerde, B. Wittmer, V. Zhukov[14]

RWTH Aachen University, III. Physikalisches Institut A, Aachen, Germany

A. Albert, D. Duchardt, M. Endres, M. Erdmann, T. Esch, R. Fischer, S. Ghosh, A. Güth, T. Hebbeker, C. Heidemann, K. Hoepfner, H. Keller, S. Knutzen, L. Mastrolorenzo, M. Merschmeyer, A. Meyer, P. Millet, S. Mukherjee, T. Pook, M. Radziej, H. Reithler, M. Rieger, F. Scheuch, A. Schmidt, D. Teyssier

RWTH Aachen University, III. Physikalisches Institut B, Aachen, Germany

G. Flügge, O. Hlushchenko, B. Kargoll, T. Kress, A. Künsken, T. Müller, A. Nehrkorn, A. Nowack, C. Pistone, O. Pooth, H. Sert, A. Stahl[16]

Deutsches Elektronen-Synchrotron, Hamburg, Germany

M. Aldaya Martin, T. Arndt, C. Asawatangtrakuldee, I. Babounikau, K. Beernaert, O. Behnke, U. Behrens, A. Bermúdez Martínez, D. Bertsche, A. A. Bin Anuar, K. Borras[17], V. Botta, A. Campbell, P. Connor, C. Contreras-Campana, F. Costanza, V. Danilov, A. De Wit, M. M. Defranchis, C. Diez Pardos, D. Domínguez Damiani, G. Eckerlin, T. Eichhorn, A. Elwood, E. Eren, E. Gallo[18], A. Geiser, J. M. Grados Luyando, A. Grohsjean, P. Gunnellini, M. Guthoff, M. Haranko, A. Harb, J. Hauk, H. Jung, M. Kasemann, J. Keaveney, C. Kleinwort, J. Knolle, D. Krücker, W. Lange, A. Lelek, T. Lenz, K. Lipka, W. Lohmann[19], R. Mankel, I.-A. Melzer-Pellmann, A. B. Meyer, M. Meyer, M. Missiroli, G. Mittag, J. Mnich, V. Myronenko, S. K. Pflitsch, D. Pitzl, A. Raspereza, M. Savitskyi, P. Saxena, P. Schütze, C. Schwanenberger, R. Shevchenko, A. Singh, N. Stefaniuk, H. Tholen, A. Vagnerini, G. P. Van Onsem, R. Walsh, Y. Wen, K. Wichmann, C. Wissing, O. Zenaiev

University of Hamburg, Hamburg, Germany

R. Aggleton, S. Bein, L. Benato, A. Benecke, V. Blobel, M. Centis Vignali, T. Dreyer, E. Garutti, D. Gonzalez, J. Haller, A. Hinzmann, A. Karavdina, G. Kasieczka, R. Klanner, R. Kogler, N. Kovalchuk, S. Kurz, V. Kutzner, J. Lange, D. Marconi, J. Multhaup, M. Niedziela, D. Nowatschin, A. Perieanu, A. Reimers, O. Rieger, C. Scharf, P. Schleper, S. Schumann, J. Schwandt, J. Sonneveld, H. Stadie, G. Steinbrück, F. M. Stober, M. Stöver, D. Troendle, A. Vanhoefer, B. Vormwald

Karlsruher Institut fuer Technology, Karlsruhe, Germany

M. Akbiyik, C. Barth, M. Baselga, S. Baur, E. Butz, R. Caspart, T. Chwalek, F. Colombo, W. De Boer, A. Dierlamm, N. Faltermann, B. Freund, M. Giffels, M. A. Harrendorf, F. Hartmann[16], S. M. Heindl, U. Husemann, F. Kassel[16], I. Katkov[14], S. Kudella, H. Mildner, S. Mitra, M. U. Mozer, Th. Müller, M. Plagge, G. Quast, K. Rabbertz, M. Schröder, I. Shvetsov, G. Sieber, H. J. Simonis, R. Ulrich, S. Wayand, M. Weber, T. Weiler, S. Williamson, C. Wöhrmann, R. Wolf

Institute of Nuclear and Particle Physics (INPP), NCSR Demokritos, Agia Paraskevi, Greece

G. Anagnostou, G. Daskalakis, T. Geralis, A. Kyriakis, D. Loukas, G. Paspalaki, I. Topsis-Giotis

National and Kapodistrian University of Athens, Athens, Greece

G. Karathanasis, S. Kesisoglou, P. Kontaxakis, A. Panagiotou, N. Saoulidou, E. Tziaferi, K. Vellidis

National Technical University of Athens, Athens, Greece

K. Kousouris, I. Papakrivopoulos, G. Tsipolitis

University of Ioánnina, Ioannina, Greece

I. Evangelou, C. Foudas, P. Gianneios, P. Katsoulis, P. Kokkas, S. Mallios, N. Manthos, I. Papadopoulos, E. Paradas, J. Strologas, F. A. Triantis, D. Tsitsonis

MTA-ELTE Lendület CMS Particle and Nuclear Physics Group, Eötvös Loránd University, Budapest, Hungary

M. Bartók[20], M. Csanad, N. Filipovic, P. Major, M. I. Nagy, G. Pasztor, O. Surányi, G. I. Veres

Wigner Research Centre for Physics, Budapest, Hungary

G. Bencze, C. Hajdu, D. Horvath[21], Á. Hunyadi, F. Sikler, T. Á. Vámi, V. Veszpremi, G. Vesztergombi[†]

Institute of Nuclear Research ATOMKI, Debrecen, Hungary

N. Beni, S. Czellar, J. Karancsi[22], A. Makovec, J. Molnar, Z. Szillasi

Institute of Physics, University of Debrecen, Debrecen, Hungary

P. Raics, Z. L. Trocsanyi, B. Ujvari

Indian Institute of Science (IISc), Bangalore, India

S. Choudhury, J. R. Komaragiri, P. C. Tiwari

National Institute of Science Education and Research, HBNI, Bhubaneswar, India

S. Bahinipati[23], C. Kar, P. Mal, K. Mandal, A. Nayak[24], D. K. Sahoo[23], S. K. Swain

Panjab University, Chandigarh, India

S. Bansal, S. B. Beri, V. Bhatnagar, S. Chauhan, R. Chawla, N. Dhingra, R. Gupta, A. Kaur, A. Kaur, M. Kaur, S. Kaur, R. Kumar, P. Kumari, M. Lohan, A. Mehta, K. Sandeep, S. Sharma, J. B. Singh, G. Walia

University of Delhi, Delhi, India

A. Bhardwaj, B. C. Choudhary, R. B. Garg, M. Gola, S. Keshri, Ashok Kumar, S. Malhotra, M. Naimuddin, P. Priyanka, K. Ranjan, Aashaq Shah, R. Sharma

Saha Institute of Nuclear Physics, HBNI, Kolkata, India

R. Bhardwaj[25], M. Bharti, R. Bhattacharya, S. Bhattacharya, U. Bhawandeep[25], D. Bhowmik, S. Dey, S. Dutt[25], S. Dutta, S. Ghosh, K. Mondal, S. Nandan, A. Purohit, P. K. Rout, A. Roy, S. Roy Chowdhury, S. Sarkar, M. Sharan, B. Singh, S. Thakur[25]

Indian Institute of Technology Madras, Madras, India

P. K. Behera

Bhabha Atomic Research Centre, Mumbai, India

R. Chudasama, D. Dutta, V. Jha, V. Kumar, P. K. Netrakanti, L. M. Pant, P. Shukla

Tata Institute of Fundamental Research-A, Mumbai, India

T. Aziz, M. A. Bhat, S. Dugad, G. B. Mohanty, N. Sur, B. Sutar, RavindraKumar Verma

Tata Institute of Fundamental Research-B, Mumbai, India

S. Banerjee, S. Bhattacharya, S. Chatterjee, P. Das, M. Guchait, Sa. Jain, S. Karmakar, S. Kumar, M. Maity[26], G. Majumder, K. Mazumdar, N. Sahoo, T. Sarkar[26]

Indian Institute of Science Education and Research (IISER), Pune, India

S. Chauhan, S. Dube, V. Hegde, A. Kapoor, K. Kothekar, S. Pandey, A. Rane, S. Sharma

Institute for Research in Fundamental Sciences (IPM), Tehran, Iran

S. Chenarani[27], E. Eskandari Tadavani, S. M. Etesami[27], M. Khakzad, M. Mohammadi Najafabadi, M. Naseri, F. Rezaei Hosseinabadi, B. Safarzadeh[28], M. Zeinali

University College Dublin, Dublin, Ireland

M. Felcini, M. Grunewald

INFN Sezione di Bari[a], Università di Bari[b], Politecnico di Bari[c], Bari, Italy

M. Abbrescia[a,b], C. Calabria[a,b], A. Colaleo[a], D. Creanza[a,c], L. Cristella[a,b], N. De Filippis[a,c], M. De Palma[a,b], A. Di Florio[a,b], F. Errico[a,b], L. Fiore[a], A. Gelmi[a,b], G. Iaselli[a,c], S. Lezki[a,b], G. Maggi[a,c], M. Maggi[a], G. Miniello[a,b], S. My[a,b], S. Nuzzo[a,b], A. Pompili[a,b], G. Pugliese[a,c], R. Radogna[a], A. Ranieri[a], G. Selvaggi[a,b], A. Sharma[a], L. Silvestris[a,16], R. Venditti[a], P. Verwilligen[a], G. Zito[a]

INFN Sezione di Bologna[a], Università di Bologna[b], Bologna, Italy

G. Abbiendi[a], C. Battilana[a,b], D. Bonacorsi[a,b], L. Borgonovi[a,b], S. Braibant-Giacomelli[a,b], R. Campanini[a,b], P. Capiluppi[a,b], A. Castro[a,b], F. R. Cavallo[a], S. S. Chhibra[a,b], C. Ciocca[a], G. Codispoti[a,b], M. Cuffiani[a,b], G. M. Dallavalle[a], F. Fabbri[a], A. Fanfani[a,b], P. Giacomelli[a], C. Grandi[a], L. Guiducci[a,b], F. Iemmi[a,b], S. Marcellini[a], G. Masetti[a], A. Montanari[a], F. L. Navarria[a,b], A. Perrotta[a], F. Primavera[a,b,16], A. M. Rossi[a,b], T. Rovelli[a,b], G. P. Siroli[a,b], N. Tosi[a]

INFN Sezione di Catania[a], Università di Catania[b], Catania, Italy

S. Albergo[a,b], A. Di Mattia[a], R. Potenza[a,b], A. Tricomi[a,b], C. Tuve[a,b]

INFN Sezione di Firenze[a], Università di Firenze[b], Firenze, Italy

G. Barbagli[a], K. Chatterjee[a,b], V. Ciulli[a,b], C. Civinini[a], R. D'Alessandro[a,b], E. Focardi[a,b], G. Latino, P. Lenzi[a,b], M. Meschini[a], S. Paoletti[a], L. Russo[a,29], G. Sguazzoni[a], D. Strom[a], L. Viliani[a]

INFN Laboratori Nazionali di Frascati, Frascati, Italy

L. Benussi, S. Bianco, F. Fabbri, D. Piccolo

INFN Sezione di Genova[a], Università di Genova[b], Genova, Italy

F. Ferro[a], F. Ravera[a,b], E. Robutti[a], S. Tosi[a,b]

INFN Sezione di Milano-Bicocca[a], Università di Milano-Bicocca[b], Milan, Italy

A. Benaglia[a], A. Beschi[b], L. Brianza[a,b], F. Brivio[a,b], V. Ciriolo[a,b,16], S. Di Guida[a,d,16], M. E. Dinardo[a,b], S. Fiorendi[a,b], S. Gennai[a], A. Ghezzi[a,b], P. Govoni[a,b], M. Malberti[a,b], S. Malvezzi[a], A. Massironi[a,b], D. Menasce[a], L. Moroni[a], M. Paganoni[a,b], D. Pedrini[a], S. Ragazzi[a,b], T. Tabarelli de Fatis[a,b]

INFN Sezione di Napoli[a], Università di Napoli 'Federico II'[b], Napoli, Italy, Università della Basilicata[c], Potenza, Italy, Università G. Marconi[d], Rome, Italy

S. Buontempo[a], N. Cavallo[a,c], A. Di Crescenzo[a,b], F. Fabozzi[a,c], F. Fienga[a], G. Galati[a], A. O. M. Iorio[a,b], W. A. Khan[a], L. Lista[a], S. Meola[a,d,16], P. Paolucci[a,16], C. Sciacca[a,b], E. Voevodina[a,b]

INFN Sezione di Padova[a], Università di Padova[b], Padova, Italy, Università di Trento[c], Trento, Italy

P. Azzi[a], N. Bacchetta[a], D. Bisello[a,b], A. Boletti[a,b], A. Bragagnolo, R. Carlin[a,b], P. Checchia[a], M. Dall'Osso[a,b], P. De Castro Manzano[a], T. Dorigo[a], U. Dosselli[a], F. Gasparini[a,b], U. Gasparini[a,b], A. Gozzelino[a], S. Lacaprara[a], P. Lujan, M. Margoni[a,b], A. T. Meneguzzo[a,b], P. Ronchese[a,b], R. Rossin[a,b], F. Simonetto[a,b], A. Tiko, E. Torassa[a], M. Zanetti[a,b], P. Zotto[a,b], G. Zumerle[a,b]

INFN Sezione di Pavia[a], Università di Pavia[b], Pavia, Italy

A. Braghieri[a], A. Magnani[a], P. Montagna[a,b], S. P. Ratti[a,b], V. Re[a], M. Ressegotti[a,b], C. Riccardi[a,b], P. Salvini[a], I. Vai[a,b], P. Vitulo[a,b]

INFN Sezione di Perugia[a], Università di Perugia[b], Perugia, Italy

L. Alunni Solestizi[a,b], M. Biasini[a,b], G. M. Bilei[a], C. Cecchi[a,b], D. Ciangottini[a,b], L. Fanò[a,b], P. Lariccia[a,b], E. Manoni[a], G. Mantovani[a,b], V. Mariani[a,b], M. Menichelli[a], A. Rossi[a,b], A. Santocchia[a,b], D. Spiga[a]

INFN Sezione di Pisa[a], Università di Pisa[b], Scuola Normale Superiore di Pisa[c], Pisa, Italy

K. Androsov[a], P. Azzurri[a], G. Bagliesi[a], L. Bianchini[a], T. Boccali[a], L. Borrello, R. Castaldi[a], M. A. Ciocci[a,b], R. Dell'Orso[a], G. Fedi[a], F. Fiori[a,c], L. Giannini[a,c], A. Giassi[a], M. T. Grippo[a], F. Ligabue[a,c], E. Manca[a,c], G. Mandorli[a,c], A. Messineo[a,b], F. Palla[a], A. Rizzi[a,b], P. Spagnolo[a], R. Tenchini[a], G. Tonelli[a,b], A. Venturi[a], P. G. Verdini[a]

INFN Sezione di Roma[a], Sapienza Università di Roma[b], Rome, Italy

L. Barone[a,b], F. Cavallari[a], M. Cipriani[a,b], N. Daci[a], D. Del Re[a,b], E. Di Marco[a,b], M. Diemoz[a], S. Gelli[a,b], E. Longo[a,b], B. Marzocchi[a,b], P. Meridiani[a], G. Organtini[a,b], F. Pandolfi[a], R. Paramatti[a,b], F. Preiato[a,b], S. Rahatlou[a,b], C. Rovelli[a], F. Santanastasio[a,b]

INFN Sezione di Torino[a], Università di Torino[b], Torino, Italy, Università del Piemonte Orientale[c], Novara, Italy

N. Amapane[a,b], R. Arcidiacono[a,c], S. Argiro[a,b], M. Arneodo[a,c], N. Bartosik[a], R. Bellan[a,b], C. Biino[a], N. Cartiglia[a], F. Cenna[a,b], S. Cometti, M. Costa[a,b], R. Covarelli[a,b], N. Demaria[a], B. Kiani[a,b], C. Mariotti[a], S. Maselli[a], E. Migliore[a,b], V. Monaco[a,b], E. Monteil[a,b], M. Monteno[a], M. M. Obertino[a,b], L. Pacher[a,b], N. Pastrone[a], M. Pelliccioni[a], G. L. Pinna Angioni[a,b], A. Romero[a,b], M. Ruspa[a,c], R. Sacchi[a,b], K. Shchelina[a], V. Sola[a], A. Solano[a,b], D. Soldi, A. Staiano[a]

INFN Sezione di Trieste[a], Università di Trieste[b], Trieste, Italy

S. Belforte[a], V. Candelise[a,b], M. Casarsa[a], F. Cossutti[a], G. Della Ricca[a,b], F. Vazzoler[a,b], A. Zanetti[a]

Kyungpook National University, Taegu, Korea

D. H. Kim, G. N. Kim, M. S. Kim, J. Lee, S. Lee, S. W. Lee, C. S. Moon, Y. D. Oh, S. Sekmen, D. C. Son, Y. C. Yang

Chonnam National University, Institute for Universe and Elementary Particles, Kwangju, Korea

H. Kim, D. H. Moon, G. Oh

Hanyang University, Seoul, Korea
J. Goh, T. J. Kim

Korea University, Seoul, Korea
S. Cho, S. Choi, Y. Go, D. Gyun, S. Ha, B. Hong, Y. Jo, K. Lee, K. S. Lee, S. Lee, J. Lim, S. K. Park, Y. Roh

Sejong University, Seoul, Korea
H. S. Kim

Seoul National University, Seoul, Korea
J. Almond, J. Kim, J. S. Kim, H. Lee, K. Lee, K. Nam, S. B. Oh, B. C. Radburn-Smith, S. h. Seo, U. K. Yang, H. D. Yoo, G. B. Yu

University of Seoul, Seoul, Korea
D. Jeon, H. Kim, J. H. Kim, J. S. H. Lee, I. C. Park

Sungkyunkwan University, Suwon, Korea
Y. Choi, C. Hwang, J. Lee, I. Yu

The Lebanese University, Beirut, Lebanon
N. Barakat[30]

Vilnius University, Vilnius, Lithuania
V. Dudenas, A. Juodagalvis, J. Vaitkus

National Centre for Particle Physics, Universiti Malaya, Kuala Lumpur, Malaysia
I. Ahmed, Z. A. Ibrahim, M. A. B. Md Ali[31], F. Mohamad Idris[32], W. A. T. Wan Abdullah, M. N. Yusli, Z. Zolkapli

Centro de Investigacion y de Estudios Avanzados del IPN, Mexico City, Mexico
H. Castilla-Valdez, E. De La Cruz-Burelo, M. C. Duran-Osuna, I. Heredia-De La Cruz[33], R. Lopez-Fernandez, J. Mejia Guisao, R. I. Rabadan-Trejo, G. Ramirez-Sanchez, R. Reyes-Almanza, A. Sanchez-Hernandez

Universidad Iberoamericana, Mexico City, Mexico
S. Carrillo Moreno, C. Oropeza Barrera, F. Vazquez Valencia

Benemerita Universidad Autonoma de Puebla, Puebla, Mexico
J. Eysermans, I. Pedraza, H. A. Salazar Ibarguen, C. Uribe Estrada

Universidad Autónoma de San Luis Potosí, San Luis Potosí, Mexico
A. Morelos Pineda

University of Auckland, Auckland, New Zealand
D. Krofcheck

University of Canterbury, Christchurch, New Zealand
S. Bheesette, P. H. Butler

National Centre for Physics, Quaid-I-Azam University, Islamabad, Pakistan
A. Ahmad, M. Ahmad, M. I. Asghar, Q. Hassan, H. R. Hoorani, A. Saddique, M. A. Shah, M. Shoaib, M. Waqas

National Centre for Nuclear Research, Swierk, Poland
H. Bialkowska, M. Bluj, B. Boimska, T. Frueboes, M. Górski, M. Kazana, K. Nawrocki, M. Szleper, P. Traczyk, P. Zalewski

Institute of Experimental Physics, Faculty of Physics, University of Warsaw, Warsaw, Poland
K. Bunkowski, A. Byszuk[34], K. Doroba, A. Kalinowski, M. Konecki, J. Krolikowski, M. Misiura, M. Olszewski, A. Pyskir, M. Walczak

Laboratório de Instrumentação e Física Experimental de Partículas, Lisbon, Portugal
P. Bargassa, C. Beirão Da Cruz E Silva, A. Di Francesco, P. Faccioli, B. Galinhas, M. Gallinaro, J. Hollar, N. Leonardo,
L. Lloret Iglesias, M. V. Nemallapudi, J. Seixas, G. Strong, O. Toldaiev, D. Vadruccio, J. Varela

Joint Institute for Nuclear Research, Dubna, Russia
A. Baginyan, A. Golunov, I. Golutvin, V. Karjavin, I. Kashunin, V. Korenkov, G. Kozlov, A. Lanev, A. Malakhov,
V. Matveev[35,36], V. V. Mitsyn, P. Moisenz, V. Palichik, V. Perelygin, S. Shmatov, N. Skatchkov, V. Smirnov,
B. S. Yuldashev[37], A. Zarubin

Petersburg Nuclear Physics Institute, Gatchina (St. Petersburg), Russia
V. Golovtsov, Y. Ivanov, V. Kim[38], E. Kuznetsova[39], P. Levchenko, V. Murzin, V. Oreshkin, I. Smirnov, D. Sosnov,
V. Sulimov, L. Uvarov, S. Vavilov, A. Vorobyev

Institute for Nuclear Research, Moscow, Russia
Yu. Andreev, A. Dermenev, S. Gninenko, N. Golubev, A. Karneyeu, M. Kirsanov, N. Krasnikov, A. Pashenkov, D. Tlisov,
A. Toropin

Institute for Theoretical and Experimental Physics, Moscow, Russia
V. Epshteyn, V. Gavrilov, N. Lychkovskaya, V. Popov, I. Pozdnyakov, G. Safronov, A. Spiridonov, A. Stepennov,
V. Stolin, M. Toms, E. Vlasov, A. Zhokin

Moscow Institute of Physics and Technology, Moscow, Russia
T. Aushev

National Research Nuclear University 'Moscow Engineering Physics Institute' (MEPhI), Moscow, Russia
M. Chadeeva[40], P. Parygin, D. Philippov, S. Polikarpov[40], E. Popova, V. Rusinov

P.N. Lebedev Physical Institute, Moscow, Russia
V. Andreev, M. Azarkin[36], I. Dremin[36], M. Kirakosyan[36], S. V. Rusakov, A. Terkulov

Skobeltsyn Institute of Nuclear Physics, Lomonosov Moscow State University, Moscow, Russia
A. Baskakov, A. Belyaev, E. Boos, M. Dubinin[41], L. Dudko, A. Ershov, A. Gribushin, V. Klyukhin, O. Kodolova,
I. Lokhtin, I. Miagkov, S. Obraztsov, S. Petrushanko, V. Savrin, A. Snigirev

Novosibirsk State University (NSU), Novosibirsk, Russia
V. Blinov[42], T. Dimova[42], L. Kardapoltsev[42], D. Shtol[42], Y. Skovpen[42]

**State Research Center of Russian Federation, Institute for High Energy Physics of NRC 'Kurchatov Institute',
Protvino, Russia**
I. Azhgirey, I. Bayshev, S. Bitioukov, D. Elumakhov, A. Godizov, V. Kachanov, A. Kalinin, D. Konstantinov, P. Mandrik,
V. Petrov, R. Ryutin, S. Slabospitskii, A. Sobol, S. Troshin, N. Tyurin, A. Uzunian, A. Volkov

National Research Tomsk Polytechnic University, Tomsk, Russia
A. Babaev, S. Baidali

University of Belgrade, Faculty of Physics and Vinca Institute of Nuclear Sciences, Belgrade, Serbia
P. Adzic[43], P. Cirkovic, D. Devetak, M. Dordevic, J. Milosevic

Centro de Investigaciones Energéticas Medioambientales y Tecnológicas (CIEMAT), Madrid, Spain
J. Alcaraz Maestre, A. Álvarez Fernández, I. Bachiller, M. Barrio Luna, J. A. Brochero Cifuentes, M. Cerrada, N. Colino,
B. De La Cruz, A. Delgado Peris, C. Fernandez Bedoya, J. P. Fernández Ramos, J. Flix, M. C. Fouz, O. Gonzalez Lopez,
S. Goy Lopez, J. M. Hernandez, M. I. Josa, D. Moran, A. Pérez-Calero Yzquierdo, J. Puerta Pelayo, I. Redondo,
L. Romero, M. S. Soares, A. Triossi

Universidad Autónoma de Madrid, Madrid, Spain
C. Albajar, J. F. de Trocóniz

Universidad de Oviedo, Oviedo, Spain

J. Cuevas, C. Erice, J. Fernandez Menendez, S. Folgueras, I. Gonzalez Caballero, J. R. González Fernández, E. Palencia Cortezon, V. Rodríguez Bouza, S. Sanchez Cruz, P. Vischia, J. M. Vizan Garcia

Instituto de Física de Cantabria (IFCA), CSIC-Universidad de Cantabria, Santander, Spain

I. J. Cabrillo, A. Calderon, B. Chazin Quero, J. Duarte Campderros, M. Fernandez, P. J. Fernández Manteca, A. García Alonso, J. Garcia-Ferrero, G. Gomez, A. Lopez Virto, J. Marco, C. Martinez Rivero, P. Martinez Ruiz del Arbol, F. Matorras, J. Piedra Gomez, C. Prieels, T. Rodrigo, A. Ruiz-Jimeno, L. Scodellaro, N. Trevisani, I. Vila, R. Vilar Cortabitarte

CERN, European Organization for Nuclear Research, Geneva, Switzerland

D. Abbaneo, B. Akgun, E. Auffray, P. Baillon, A. H. Ball, D. Barney, J. Bendavid, M. Bianco, A. Bocci, C. Botta, T. Camporesi, M. Cepeda, G. Cerminara, E. Chapon, Y. Chen, G. Cucciati, D. d'Enterria, A. Dabrowski, V. Daponte, A. David, A. De Roeck, N. Deelen, M. Dobson, T. du Pree, M. Dünser, N. Dupont, A. Elliott-Peisert, P. Everaerts, F. Fallavollita[44], D. Fasanella, G. Franzoni, J. Fulcher, W. Funk, D. Gigi, A. Gilbert, K. Gill, F. Glege, M. Guilbaud, D. Gulhan, J. Hegeman, V. Innocente, A. Jafari, P. Janot, O. Karacheban[19], J. Kieseler, A. Kornmayer, M. Krammer[1], C. Lange, P. Lecoq, C. Lourenço, L. Malgeri, M. Mannelli, F. Meijers, J. A. Merlin, S. Mersi, E. Meschi, P. Milenovic[45], F. Moortgat, M. Mulders, J. Ngadiuba, S. Orfanelli, L. Orsini, F. Pantaleo[16], L. Pape, E. Perez, M. Peruzzi, A. Petrilli, G. Petrucciani, A. Pfeiffer, M. Pierini, F. M. Pitters, D. Rabady, A. Racz, T. Reis, G. Rolandi[46], M. Rovere, H. Sakulin, C. Schäfer, C. Schwick, M. Seidel, M. Selvaggi, A. Sharma, P. Silva, P. Sphicas[47], A. Stakia, J. Steggemann, M. Tosi, D. Treille, A. Tsirou, V. Veckalns[48], W. D. Zeuner

Paul Scherrer Institut, Villigen, Switzerland

L. Caminada[49], K. Deiters, W. Erdmann, R. Horisberger, Q. Ingram, H. C. Kaestli, D. Kotlinski, U. Langenegger, T. Rohe, S. A. Wiederkehr

ETH Zurich-Institute for Particle Physics and Astrophysics (IPA), Zurich, Switzerland

M. Backhaus, L. Bäni, P. Berger, N. Chernyavskaya, G. Dissertori, M. Dittmar, M. Donegà, C. Dorfer, C. Grab, C. Heidegger, D. Hits, J. Hoss, T. Klijnsma, W. Lustermann, R. A. Manzoni, M. Marionneau, M. T. Meinhard, F. Micheli, P. Musella, F. Nessi-Tedaldi, J. Pata, F. Pauss, G. Perrin, L. Perrozzi, S. Pigazzini, M. Quittnat, D. Ruini, D. A. Sanz Becerra, M. Schönenberger, L. Shchutska, V. R. Tavolaro, K. Theofilatos, M. L. Vesterbacka Olsson, R. Wallny, D. H. Zhu

Universität Zürich, Zurich, Switzerland

T. K. Aarrestad, C. Amsler[50], D. Brzhechko, M. F. Canelli, A. De Cosa, R. Del Burgo, S. Donato, C. Galloni, T. Hreus, B. Kilminster, I. Neutelings, D. Pinna, G. Rauco, P. Robmann, D. Salerno, K. Schweiger, C. Seitz, Y. Takahashi, A. Zucchetta

National Central University, Chung-Li, Taiwan

Y. H. Chang, K. y. Cheng, T. H. Doan, Sh. Jain, R. Khurana, C. M. Kuo, W. Lin, A. Pozdnyakov, S. S. Yu

National Taiwan University (NTU), Taipei, Taiwan

P. Chang, Y. Chao, K. F. Chen, P. H. Chen, W.-S. Hou, Arun Kumar, Y. y. Li, R.-S. Lu, E. Paganis, A. Psallidas, A. Steen, J. f. Tsai

Chulalongkorn University, Faculty of Science, Department of Physics, Bangkok, Thailand

B. Asavapibhop, N. Srimanobhas, N. Suwonjandee

Çukurova University, Physics Department, Science and Art Faculty, Adana, Turkey

A. Bat, F. Boran, S. Cerci[51], S. Damarseckin, Z. S. Demiroglu, F. Dolek, C. Dozen, I. Dumanoglu, S. Girgis, G. Gokbulut, Y. Guler, E. Gurpinar, I. Hos[52], C. Isik, E. E. Kangal[53], O. Kara, A. Kayis Topaksu, U. Kiminsu, M. Oglakci, G. Onengut, K. Ozdemir[54], S. Ozturk[55], D. Sunar Cerci[51], B. Tali[51], U. G. Tok, S. Turkcapar, I. S. Zorbakir, C. Zorbilmez

Middle East Technical University, Physics Department, Ankara, Turkey

B. Isildak[56], G. Karapinar[57], M. Yalvac, M. Zeyrek

Bogazici University, Istanbul, Turkey

I. O. Atakisi, E. Gülmez, M. Kaya[58], O. Kaya[59], S. Tekten, E. A. Yetkin[60]

Istanbul Technical University, Istanbul, Turkey
M. N. Agaras, S. Atay, A. Cakir, K. Cankocak, Y. Komurcu, S. Sen[61]

Institute for Scintillation Materials of National Academy of Science of Ukraine, Kharkov, Ukraine
B. Grynyov

National Scientific Center, Kharkov Institute of Physics and Technology, Kharkov, Ukraine
L. Levchuk

University of Bristol, Bristol, UK
F. Ball, L. Beck, J. J. Brooke, D. Burns, E. Clement, D. Cussans, O. Davignon, H. Flacher, J. Goldstein, G. P. Heath, H. F. Heath, L. Kreczko, D. M. Newbold[62], S. Paramesvaran, B. Penning, T. Sakuma, D. Smith, V. J. Smith, J. Taylor, A. Titterton

Rutherford Appleton Laboratory, Didcot, UK
K. W. Bell, A. Belyaev[63], C. Brew, R. M. Brown, D. Cieri, D. J. A. Cockerill, J. A. Coughlan, K. Harder, S. Harper, J. Linacre, E. Olaiya, D. Petyt, C. H. Shepherd-Themistocleous, A. Thea, I. R. Tomalin, T. Williams, W. J. Womersley

Imperial College, London, UK
G. Auzinger, R. Bainbridge, P. Bloch, J. Borg, S. Breeze, O. Buchmuller, A. Bundock, S. Casasso, D. Colling, L. Corpe, P. Dauncey, G. Davies, M. Della Negra, R. Di Maria, Y. Haddad, G. Hall, G. Iles, T. James, M. Komm, C. Laner, L. Lyons, A.-M. Magnan, S. Malik, A. Martelli, J. Nash[64], A. Nikitenko[6], V. Palladino, M. Pesaresi, A. Richards, A. Rose, E. Scott, C. Seez, A. Shtipliyski, G. Singh, M. Stoye, T. Strebler, S. Summers, A. Tapper, K. Uchida, T. Virdee[16], N. Wardle, D. Winterbottom, J. Wright, S. C. Zenz

Brunel University, Uxbridge, UK
J. E. Cole, P. R. Hobson, A. Khan, P. Kyberd, C. K. Mackay, A. Morton, I. D. Reid, L. Teodorescu, S. Zahid

Baylor University, Waco, USA
K. Call, J. Dittmann, K. Hatakeyama, H. Liu, C. Madrid, B. Mcmaster, N. Pastika, C. Smith

Catholic University of America, Washington, DC, USA
R. Bartek, A. Dominguez

The University of Alabama, Tuscaloosa, USA
A. Buccilli, S. I. Cooper, C. Henderson, P. Rumerio, C. West

Boston University, Boston, USA
D. Arcaro, T. Bose, D. Gastler, D. Rankin, C. Richardson, J. Rohlf, L. Sulak, D. Zou

Brown University, Providence, USA
G. Benelli, X. Coubez, D. Cutts, M. Hadley, J. Hakala, U. Heintz, J. M. Hogan[65], K. H. M. Kwok, E. Laird, G. Landsberg, J. Lee, Z. Mao, M. Narain, J. Pazzini, S. Piperov, S. Sagir[66], R. Syarif, E. Usai, D. Yu

University of California, Davis, Davis, USA
R. Band, C. Brainerd, R. Breedon, D. Burns, M. Calderon De La Barca Sanchez, M. Chertok, J. Conway, R. Conway, P. T. Cox, R. Erbacher, C. Flores, G. Funk, W. Ko, O. Kukral, R. Lander, C. Mclean, M. Mulhearn, D. Pellett, J. Pilot, S. Shalhout, M. Shi, D. Stolp, D. Taylor, K. Tos, M. Tripathi, Z. Wang, F. Zhang

University of California, Los Angeles, USA
M. Bachtis, C. Bravo, R. Cousins, A. Dasgupta, A. Florent, J. Hauser, M. Ignatenko, N. Mccoll, S. Regnard, D. Saltzberg, C. Schnaible, V. Valuev

University of California, Riverside, Riverside, USA
E. Bouvier, K. Burt, R. Clare, J. W. Gary, S. M. A. Ghiasi Shirazi, G. Hanson, G. Karapostoli, E. Kennedy, F. Lacroix, O. R. Long, M. Olmedo Negrete, M. I. Paneva, W. Si, L. Wang, H. Wei, S. Wimpenny, B. R. Yates

University of California, San Diego, La Jolla, USA

J. G. Branson, S. Cittolin, M. Derdzinski, R. Gerosa, D. Gilbert, B. Hashemi, A. Holzner, D. Klein, G. Kole, V. Krutelyov, J. Letts, M. Masciovecchio, D. Olivito, S. Padhi, M. Pieri, M. Sani, V. Sharma, S. Simon, M. Tadel, A. Vartak, S. Wasserbaech[67], J. Wood, F. Würthwein, A. Yagil, G. Zevi Della Porta

Department of Physics, University of California, Santa Barbara, Santa Barbara, USA

N. Amin, R. Bhandari, J. Bradmiller-Feld, C. Campagnari, M. Citron, A. Dishaw, V. Dutta, M. Franco Sevilla, L. Gouskos, R. Heller, J. Incandela, A. Ovcharova, H. Qu, J. Richman, D. Stuart, I. Suarez, S. Wang, J. Yoo

California Institute of Technology, Pasadena, USA

D. Anderson, A. Bornheim, J. M. Lawhorn, H. B. Newman, T. Q. Nguyen, M. Spiropulu, J. R. Vlimant, R. Wilkinson, S. Xie, Z. Zhang, R. Y. Zhu

Carnegie Mellon University, Pittsburgh, USA

M. B. Andrews, T. Ferguson, T. Mudholkar, M. Paulini, M. Sun, I. Vorobiev, M. Weinberg

University of Colorado Boulder, Boulder, USA

J. P. Cumalat, W. T. Ford, F. Jensen, A. Johnson, M. Krohn, S. Leontsinis, E. MacDonald, T. Mulholland, K. Stenson, K. A. Ulmer, S. R. Wagner

Cornell University, Ithaca, USA

J. Alexander, J. Chaves, Y. Cheng, J. Chu, A. Datta, K. Mcdermott, N. Mirman, J. R. Patterson, D. Quach, A. Rinkevicius, A. Ryd, L. Skinnari, L. Soffi, S. M. Tan, Z. Tao, J. Thom, J. Tucker, P. Wittich, M. Zientek

Fermi National Accelerator Laboratory, Batavia, USA

S. Abdullin, M. Albrow, M. Alyari, G. Apollinari, A. Apresyan, A. Apyan, S. Banerjee, L. A. T. Bauerdick, A. Beretvas, J. Berryhill, P. C. Bhat, G. Bolla[†], K. Burkett, J. N. Butler, A. Canepa, G. B. Cerati, H. W. K. Cheung, F. Chlebana, M. Cremonesi, J. Duarte, V. D. Elvira, J. Freeman, Z. Gecse, E. Gottschalk, L. Gray, D. Green, S. Grünendahl, O. Gutsche, J. Hanlon, R. M. Harris, S. Hasegawa, J. Hirschauer, Z. Hu, B. Jayatilaka, S. Jindariani, M. Johnson, U. Joshi, B. Klima, M. J. Kortelainen, B. Kreis, S. Lammel, D. Lincoln, R. Lipton, M. Liu, T. Liu, J. Lykken, K. Maeshima, J. M. Marraffino, D. Mason, P. McBride, P. Merkel, S. Mrenna, S. Nahn, V. O'Dell, K. Pedro, C. Pena, O. Prokofyev, G. Rakness, L. Ristori, A. Savoy-Navarro[68], B. Schneider, E. Sexton-Kennedy, A. Soha, W. J. Spalding, L. Spiegel, S. Stoynev, J. Strait, N. Strobbe, L. Taylor, S. Tkaczyk, N. V. Tran, L. Uplegger, E. W. Vaandering, C. Vernieri, M. Verzocchi, R. Vidal, M. Wang, H. A. Weber, A. Whitbeck

University of Florida, Gainesville, USA

D. Acosta, P. Avery, P. Bortignon, D. Bourilkov, A. Brinkerhoff, L. Cadamuro, A. Carnes, M. Carver, D. Curry, R. D. Field, S. V. Gleyzer, B. M. Joshi, J. Konigsberg, A. Korytov, P. Ma, K. Matchev, H. Mei, G. Mitselmakher, K. Shi, D. Sperka, J. Wang, S. Wang

Florida International University, Miami, USA

Y. R. Joshi, S. Linn

Florida State University, Tallahassee, USA

A. Ackert, T. Adams, A. Askew, S. Hagopian, V. Hagopian, K. F. Johnson, T. Kolberg, G. Martinez, T. Perry, H. Prosper, A. Saha, A. Santra, V. Sharma, R. Yohay

Florida Institute of Technology, Melbourne, USA

M. M. Baarmand, V. Bhopatkar, S. Colafranceschi, M. Hohlmann, D. Noonan, M. Rahmani, T. Roy, F. Yumiceva

University of Illinois at Chicago (UIC), Chicago, USA

M. R. Adams, L. Apanasevich, D. Berry, R. R. Betts, R. Cavanaugh, X. Chen, S. Dittmer, O. Evdokimov, C. E. Gerber, D. A. Hangal, D. J. Hofman, K. Jung, J. Kamin, C. Mills, I. D. Sandoval Gonzalez, M. B. Tonjes, N. Varelas, H. Wang, X. Wang, Z. Wu, J. Zhang

The University of Iowa, Iowa City, USA

M. Alhusseini, B. Bilki[69], W. Clarida, K. Dilsiz[70], S. Durgut, R. P. Gandrajula, M. Haytmyradov, V. Khristenko, J.-P. Merlo, A. Mestvirishvili, A. Moeller, J. Nachtman, H. Ogul[71], Y. Onel, F. Ozok[72], A. Penzo, C. Snyder, E. Tiras, J. Wetzel

Johns Hopkins University, Baltimore, USA

B. Blumenfeld, A. Cocoros, N. Eminizer, D. Fehling, L. Feng, A. V. Gritsan, W. T. Hung, P. Maksimovic, J. Roskes, U. Sarica, M. Swartz, M. Xiao, C. You

The University of Kansas, Lawrence, USA

A. Al-bataineh, P. Baringer, A. Bean, S. Boren, J. Bowen, A. Bylinkin, J. Castle, S. Khalil, A. Kropivnitskaya, D. Majumder, W. Mcbrayer, M. Murray, C. Rogan, S. Sanders, E. Schmitz, J. D. Tapia Takaki, Q. Wang

Kansas State University, Manhattan, USA

A. Ivanov, K. Kaadze, D. Kim, Y. Maravin, D. R. Mendis, T. Mitchell, A. Modak, A. Mohammadi, L. K. Saini, N. Skhirtladze

Lawrence Livermore National Laboratory, Livermore, USA

F. Rebassoo, D. Wright

University of Maryland, College Park, USA

A. Baden, O. Baron, A. Belloni, S. C. Eno, Y. Feng, C. Ferraioli, N. J. Hadley, S. Jabeen, G. Y. Jeng, R. G. Kellogg, J. Kunkle, A. C. Mignerey, F. Ricci-Tam, Y. H. Shin, A. Skuja, S. C. Tonwar, K. Wong

Massachusetts Institute of Technology, Cambridge, USA

D. Abercrombie, B. Allen, V. Azzolini, A. Baty, G. Bauer, R. Bi, S. Brandt, W. Busza, I. A. Cali, M. D'Alfonso, Z. Demiragli, G. Gomez Ceballos, M. Goncharov, P. Harris, D. Hsu, M. Hu, Y. Iiyama, G. M. Innocenti, M. Klute, D. Kovalskyi, Y.-J. Lee, P. D. Luckey, B. Maier, A. C. Marini, C. Mcginn, C. Mironov, S. Narayanan, X. Niu, C. Paus, C. Roland, G. Roland, G. S. F. Stephans, K. Sumorok, K. Tatar, D. Velicanu, J. Wang, T. W. Wang, B. Wyslouch, S. Zhaozhong

University of Minnesota, Minneapolis, USA

A. C. Benvenuti, R. M. Chatterjee, A. Evans, P. Hansen, S. Kalafut, Y. Kubota, Z. Lesko, J. Mans, S. Nourbakhsh, N. Ruckstuhl, R. Rusack, J. Turkewitz, M. A. Wadud

University of Mississippi, Oxford, USA

J. G. Acosta, S. Oliveros

University of Nebraska-Lincoln, Lincoln, USA

E. Avdeeva, K. Bloom, D. R. Claes, C. Fangmeier, F. Golf, R. Gonzalez Suarez, R. Kamalieddin, I. Kravchenko, J. Monroy, J. E. Siado, G. R. Snow, B. Stieger

State University of New York at Buffalo, Buffalo, USA

A. Godshalk, C. Harrington, I. Iashvili, A. Kharchilava, D. Nguyen, A. Parker, S. Rappoccio, B. Roozbahani

Northeastern University, Boston, USA

G. Alverson, E. Barberis, C. Freer, A. Hortiangtham, D. M. Morse, T. Orimoto, R. Teixeira De Lima, T. Wamorkar, B. Wang, A. Wisecarver, D. Wood

Northwestern University, Evanston, USA

S. Bhattacharya, O. Charaf, K. A. Hahn, N. Mucia, N. Odell, M. H. Schmitt, K. Sung, M. Trovato, M. Velasco

University of Notre Dame, Notre Dame, USA

R. Bucci, N. Dev, M. Hildreth, K. Hurtado Anampa, C. Jessop, D. J. Karmgard, N. Kellams, K. Lannon, W. Li, N. Loukas, N. Marinelli, F. Meng, C. Mueller, Y. Musienko[35], M. Planer, A. Reinsvold, R. Ruchti, P. Siddireddy, G. Smith, S. Taroni, M. Wayne, A. Wightman, M. Wolf, A. Woodard

The Ohio State University, Columbus, USA

J. Alimena, L. Antonelli, B. Bylsma, L. S. Durkin, S. Flowers, B. Francis, A. Hart, C. Hill, W. Ji, T. Y. Ling, W. Luo, B. L. Winer, H. W. Wulsin

Princeton University, Princeton, USA

S. Cooperstein, P. Elmer, J. Hardenbrook, P. Hebda, S. Higginbotham, A. Kalogeropoulos, D. Lange, M. T. Lucchini, J. Luo, D. Marlow, K. Mei, I. Ojalvo, J. Olsen, C. Palmer, P. Piroué, J. Salfeld-Nebgen, D. Stickland, C. Tully

University of Puerto Rico, Mayaguez, USA

S. Malik, S. Norberg

Purdue University, West Lafayette, USA

A. Barker, V. E. Barnes, S. Das, L. Gutay, M. Jones, A. W. Jung, A. Khatiwada, B. Mahakud, D. H. Miller, N. Neumeister, C. C. Peng, H. Qiu, J. F. Schulte, J. Sun, F. Wang, R. Xiao, W. Xie

Purdue University Northwest, Hammond, USA

T. Cheng, J. Dolen, N. Parashar

Rice University, Houston, USA

Z. Chen, K. M. Ecklund, S. Freed, F. J. M. Geurts, M. Kilpatrick, W. Li, B. Michlin, B. P. Padley, J. Roberts, J. Rorie, W. Shi, Z. Tu, J. Zabel, A. Zhang

University of Rochester, Rochester, USA

A. Bodek, P. de Barbaro, R. Demina, Y. t. Duh, J. L. Dulemba, C. Fallon, T. Ferbel, M. Galanti, A. Garcia-Bellido, J. Han, O. Hindrichs, A. Khukhunaishvili, K. H. Lo, P. Tan, R. Taus, M. Verzetti

Rutgers, The State University of New Jersey, Piscataway, USA

A. Agapitos, J. P. Chou, Y. Gershtein, T. A. Gómez Espinosa, E. Halkiadakis, M. Heindl, E. Hughes, S. Kaplan, R. Kunnawalkam Elayavalli, S. Kyriacou, A. Lath, R. Montalvo, K. Nash, M. Osherson, H. Saka, S. Salur, S. Schnetzer, D. Sheffield, S. Somalwar, R. Stone, S. Thomas, P. Thomassen, M. Walker

University of Tennessee, Knoxville, USA

A. G. Delannoy, J. Heideman, G. Riley, K. Rose, S. Spanier, K. Thapa

Texas A & M University, College Station, USA

O. Bouhali[73], A. Castaneda Hernandez[73], A. Celik, M. Dalchenko, M. De Mattia, A. Delgado, S. Dildick, R. Eusebi, J. Gilmore, T. Huang, T. Kamon[74], S. Luo, R. Mueller, Y. Pakhotin, R. Patel, A. Perloff, L. Perniè, D. Rathjens, A. Safonov, A. Tatarinov

Texas Tech University, Lubbock, USA

N. Akchurin, J. Damgov, F. De Guio, P. R. Dudero, S. Kunori, K. Lamichhane, S. W. Lee, T. Mengke, S. Muthumuni, T. Peltola, S. Undleeb, I. Volobouev, Z. Wang

Vanderbilt University, Nashville, USA

S. Greene, A. Gurrola, R. Janjam, W. Johns, C. Maguire, A. Melo, H. Ni, K. Padeken, J. D. Ruiz Alvarez, P. Sheldon, S. Tuo, J. Velkovska, M. Verweij, Q. Xu

University of Virginia, Charlottesville, USA

M. W. Arenton, P. Barria, B. Cox, R. Hirosky, M. Joyce, A. Ledovskoy, H. Li, C. Neu, T. Sinthuprasith, Y. Wang, E. Wolfe, F. Xia

Wayne State University, Detroit, USA

R. Harr, P. E. Karchin, N. Poudyal, J. Sturdy, P. Thapa, S. Zaleski

University of Wisconsin-Madison, Madison, WI, USA

M. Brodski, J. Buchanan, C. Caillol, D. Carlsmith, S. Dasu, L. Dodd, S. Duric, B. Gomber, M. Grothe, M. Herndon, A. Hervé, U. Hussain, P. Klabbers, A. Lanaro, A. Levine, K. Long, R. Loveless, T. Ruggles, A. Savin, N. Smith, W. H. Smith, N. Woods

† **Deceased**

1: Also at Vienna University of Technology, Vienna, Austria
2: Also at IRFU, CEA, Université Paris-Saclay, Gif-sur-Yvette, France
3: Also at Universidade Estadual de Campinas, Campinas, Brazil

4: Also at Federal University of Rio Grande do Sul, Porto Alegre, Brazil

5: Also at Université Libre de Bruxelles, Bruxelles, Belgium

6: Also at Institute for Theoretical and Experimental Physics, Moscow, Russia

7: Also at Joint Institute for Nuclear Research, Dubna, Russia

8: Now at Cairo University, Cairo, Egypt

9: Also at Fayoum University, El-Fayoum, Egypt

10: Now at British University in Egypt, Cairo, Egypt

11: Now at Ain Shams University, Cairo, Egypt

12: Also at Department of Physics, King Abdulaziz University, Jeddah, Saudi Arabia

13: Also at Université de Haute Alsace, Mulhouse, France

14: Also at Skobeltsyn Institute of Nuclear Physics, Lomonosov Moscow State University, Moscow, Russia

15: Also at Tbilisi State University, Tbilisi, Georgia

16: Also at CERN, European Organization for Nuclear Research, Geneva, Switzerland

17: Also at RWTH Aachen University, III. Physikalisches Institut A, Aachen, Germany

18: Also at University of Hamburg, Hamburg, Germany

19: Also at Brandenburg University of Technology, Cottbus, Germany

20: Also at MTA-ELTE Lendület CMS Particle and Nuclear Physics Group, Eötvös Loránd University, Budapest, Hungary

21: Also at Institute of Nuclear Research ATOMKI, Debrecen, Hungary

22: Also at Institute of Physics, University of Debrecen, Debrecen, Hungary

23: Also at Indian Institute of Technology Bhubaneswar, Bhubaneswar, India

24: Also at Institute of Physics, Bhubaneswar, India

25: Also at Shoolini University, Solan, India

26: Also at University of Visva-Bharati, Santiniketan, India

27: Also at Isfahan University of Technology, Isfahan, Iran

28: Also at Plasma Physics Research Center, Science and Research Branch, Islamic Azad University, Tehran, Iran

29: Also at Università degli Studi di Siena, Siena, Italy

30: Also at Universiteit Antwerpen, Antwerpen, Belgium

31: Also at International Islamic University of Malaysia, Kuala Lumpur, Malaysia

32: Also at Malaysian Nuclear Agency, MOSTI, Kajang, Malaysia

33: Also at Consejo Nacional de Ciencia y Tecnología, Mexico city, Mexico

34: Also at Warsaw University of Technology, Institute of Electronic Systems, Warsaw, Poland

35: Also at Institute for Nuclear Research, Moscow, Russia

36: Now at National Research Nuclear University 'Moscow Engineering Physics Institute' (MEPhI), Moscow, Russia

37: Also at Institute of Nuclear Physics of the Uzbekistan Academy of Sciences, Tashkent, Uzbekistan

38: Also at St. Petersburg State Polytechnical University, St. Petersburg, Russia

39: Also at University of Florida, Gainesville, USA

40: Also at P.N. Lebedev Physical Institute, Moscow, Russia

41: Also at California Institute of Technology, Pasadena, USA

42: Also at Budker Institute of Nuclear Physics, Novosibirsk, Russia

43: Also at Faculty of Physics, University of Belgrade, Belgrade, Serbia

44: Also at INFN Sezione di Pavia^a, Università di Pavia^b, Pavia, Italy

45: Also at University of Belgrade, Faculty of Physics and Vinca Institute of Nuclear Sciences, Belgrade, Serbia

46: Also at Scuola Normale e Sezione dell'INFN, Pisa, Italy

47: Also at National and Kapodistrian University of Athens, Athens, Greece

48: Also at Riga Technical University, Riga, Latvia

49: Also at Universität Zürich, Zurich, Switzerland

50: Also at Stefan Meyer Institute for Subatomic Physics (SMI), Vienna, Austria

51: Also at Adiyaman University, Adiyaman, Turkey

52: Also at Istanbul Aydin University, Istanbul, Turkey

53: Also at Mersin University, Mersin, Turkey

54: Also at Piri Reis University, Istanbul, Turkey

55: Also at Gaziosmanpasa University, Tokat, Turkey

56: Also at Ozyegin University, Istanbul, Turkey

57: Also at Izmir Institute of Technology, Izmir, Turkey

58: Also at Marmara University, Istanbul, Turkey

59: Also at Kafkas University, Kars, Turkey

60: Also at Istanbul Bilgi University, Istanbul, Turkey

61: Also at Hacettepe University, Ankara, Turkey

62: Also at Rutherford Appleton Laboratory, Didcot, UK

63: Also at School of Physics and Astronomy, University of Southampton, Southampton, UK

64: Also at Monash University, Faculty of Science, Clayton, Australia

65: Also at Bethel University, St. Paul, USA

66: Also at Karamanoğlu Mehmetbey University, Karaman, Turkey

67: Also at Utah Valley University, Orem, USA

68: Also at Purdue University, West Lafayette, USA

69: Also at Beykent University, Istanbul, Turkey

70: Also at Bingol University, Bingol, Turkey

71: Also at Sinop University, Sinop, Turkey

72: Also at Mimar Sinan University, Istanbul, Istanbul, Turkey

73: Also at Texas A&M University at Qatar, Doha, Qatar

74: Also at Kyungpook National University, Daegu, Korea